Master of Science Thesis in Electrical Engineering
Department of Electrical Engineering, Linköping University, 2022

Evaluation of models and Optimisation Methods for Energy Minimisation of Drill Riggs

Max Olsson & Mohamed Faraj

Master of Science Thesis in Electrical Engineering

Evaluation of models and Optimisation Methods for Energy Minimisation of Drill Riggs

Max Olsson & Mohamed Faraj

LiTH-ISY-EX--22/5515--SE

Supervisor: **Arvind Balachandran**
ISY, Linköpings universitet
Prabhu Bernard
Epiroc Rock Drills AB

Examiner: **Mattias Krysander**
ISY, Linköpings universitet

Division of Vehicular Systems
Department of Electrical Engineering
Linköping University
SE-581 83 Linköping, Sweden

Abstract

There are many benefits from using electrical powertrains over diesel powertrains within the mining industries, where some of these benefits come from reducing the pollution within the mines and therefore improve the working environment as well as reduce the ventilation costs required from ventilating these pollution.

It is also desired to optimise the use of the vehicle to increase the efficiency and reduce fuel consumption of the vehicle. This thesis models a boomer, a face drilling rig for underground mining, from Epiroc as well as provides optimisation methods that can be used to both optimise the model parameters to match the physical machine as well as optimise the use of the vehicle. The optimisation methods used within this thesis is non-linear programming by quadratic lagrangian optimisation, genetic algorithm optimisation as well as deterministic dynamic programming optimisation.

The results shows that with the use of these optimisation methods, models can be created to accurately be matched to a physical machine. Furthermore, vehicle component optimisation and speed optimisation can be done to lower the consumed energy as well as increase the system efficiency.

Acknowledgments

First of all we would like to express our gratitude to Epiroc for giving us this master thesis opportunity. Especially Prabhu Bernard for support throughout this thesis and your support have been helpful. We also would like to thank Gunnar Lantz from Siemens for all the support related to AMEsim.

From the university we would like to give our thanks to Arvind Balachandran for very valuable inputs throughout the master thesis.

Linköping, June 2022
Max Olsson and Mohamed Faraj

Contents

Notation

Nomenclature

Notation	Meaning
N	rotational speed
Q	flow rate
f_t	vehicle traction force
f_I	vehicle inertial load
f_r	wheel rolling resistance
f_g	gravitational force
ρ_g	gearbox efficiency
ρ_a	air resistance
ρ_e	electrical motor efficiency
$\mathbb{R}$	real number
u	clutch signal
m_v	vehicle mass
A_f	vehicle frontal area
c_d	air resistance
c_r	rolling resistance
α	slope angle
g	gravity
ω_m	motor generated rotational speed
T_m	motor generated torque
I_m	motor current
T_{gb}	Gearbox generated torque
ω_{gb}	gearbox generated rotational speed
G_{gb}	Gearbox ratio
η_{gb}	gearbox efficiency
I_{gb}	gearbox inertia
T_d	differential generated torque
ω_d	differential generated rotational speed
G_d	differential gear ratio

Nomenclature - continuation

Notation	Meaning
η_d	differential efficiency
T_w	wheel torque
I_w	wheel inertia
ω_w	wheel rotational speed
U_b	motor voltage
I_b	motor current
P_b	motor electrical power
Q_0	initial battery charge
Q	battery charge
$U_{battery}$	battery voltage
SR	standard resistance
R_{int}	internal resistance
C	C-rate
d_{range}	range of a drive cycle
E_{cycle}	energy consumed by a cycle in the drive cycle
SOC_{max}	maximum allowed soc
SOC_{min}	minimum allowed soc
t_f	depleted battery time
AC	alternating current
DC	direct current
η_m	motor efficiency map
η_b	battery efficiency
η_g	generator efficiency map
γ_{tot}	total vehicle transmission ratio
r_w	wheel radius
v_{max}	maximum vehicle speed
t_{req}	required time to finish a drive cycle
f	friction
ρ_{air}	air density
C_{stick}	stick coefficient
γ	gear ratio
c_m	continuous maximum motor speed
d_p	torque converter pump diameter
ρ_{tc}	torque converter fluid density
θ_{tc}	torque converter efficiency
S_p	sensitivity factor
p	sensitivity parameter
N_r	number of cogs on ring gear
N_s	number of cogs on sun gear
S	sun gear
C	carrier
R	ring gear

Nomenclature - continuation

Notation	Meaning
η_{sr}	efficiency between sun and ring gear
m_{gsr}	mass of planetary gear
Θ_v	total inertia after torque converter
e	induced electromagnetic force
I_m	current waveform amplitude
E_m	back EMF waveform amplitude
ω	current angular velocity
Θ	phase difference between the current and back EMF waveforms
i	the sinusoidal phase current
ω_m	motor rotating speed

Abbreviations

Abbreviation	Meaning
EV	Electrical Vehicle
PM	Permanent Magnet
PMSM	Permanent Magnet Synchronous Motor
SOC	State of charge
QSS	Quasi static approach
ODE	Ordinary differential equation
OCV	Open circuit voltage
BT	Battery
PB	Power converter
EM	Electrical motor
GB	Gear box
DDP	Deterministic dynamic programming
NLP	Non-linear optimisation problems
NLPQL	Non-linear programming by quadratic langrangian
QP	Quadratic programming
SQP	Sequential quadratic programming
DOF	Degree of freedom

1

Introduction

This master thesis is performed during the spring of 2022 at Epiroc Rock Drills in Örebro. Epiroc is a leading supplier of mining and rock quarrying equipment and offers a wide range of world class products used worldwide. Their products include drill rigs, loaders, trucks, ventilation systems, rock reinforcement, material handling etcetera. An important part of Epiroc's work is sustainability and they therefore work towards mining with the help of battery-powered, emission-free equipment to minimise environmental impact and create a healthy working environment. Epiroc currently have a fleet of electrified vehicles and are to expand their emission-free solutions, which also is the main area of this master thesis.

This master thesis is about developing a simulation model for their electrical powertrain on drill rigs as well provide Epiroc with methods that with the use of different optimisation algorithms can both match the model with the physical machine as well as optimise the use of the physical machine.

1.1 Boomer

The boomer series is a face drilling rig where the boomer weight approximately 12 600 kg and the available test vehicle weight between 18 000 and 21 000 kg depending on configuration choices. A drill rig with one boom, shown in Figure 1.1 was chosen from the portfolio to base the development of simulation models.

Figure 1.1: *Drill rig with one boomer.*

1.2 Motivation

The reason of why Epiroc is introducing electrical machines is due to its many benefits. These benefits include both improved environmental impact and health and safety environment for the operators [1]. Another part is that one of the greatest costs of any mine is the ventilation needed, and using electrical machines can reduce this cost in half.
Apart from the health perspective, using simulations speeds up the time to market process of a product since there is no need to create a new prototype for changes in the product since a change can easily be implemented in the model and quickly evaluated. It also reduces the cost due to no need to create and destroy expensive prototypes. With this model, different components can be changed or implemented in a short amount of time without huge cost.

1.3 Purpose

The purpose of this thesis is to easier test and evaluate new components in regard of the efficiency and energy consumption of a EV powertrain and to use the model to improve the efficiency of the powertrain as well as provide methods to optimise parameters and speed trajectory.

1.4 Problem description

This master thesis consist of three main parts as can be seen in Figure 1.2. The first part of this master thesis is to create a electrical corresponding simulation model for the propulsion system to a available test vehicle which can be used to validate the simulation model. This model will be validated and tuned towards physical test data. By providing the vehicle model with the same input data as the physical machine, the model can be validated and modified to match the output data measured from the physical machine. Some parameters are unknown and needs to be estimated using physical test data and optimisation methods. Thus a evaluation is done on how genetic algorithm and non-linear programming by quadratic langrangian (NLPQL) can be used to estimate the parameters. Therefore the question is:

- Evaluate how genetic algorithm and NLPQL optimisation can be used to estimate unknown model parameters with physical machine?

The second part of the master thesis is to implement a corresponding simulation model for the boomer, by changing some model parameters. The results can be used to improve the existing battery and motor sizing methodologies. When this is done, this model will be modified for use of either a centralised motor, axle motors or hub motors, and ready to be used by Epiroc to test the efficiency for the different configurations. Thereafter, NLPQL optimisation is evaluated for component selection to increase the efficiency and minimise the energy consumption in a drive cycle. Therefore the following question is:

- Evaluate how a NLPQL optimisation method can be used when selecting vehicle components to increase the efficiency and minimise the consumed energy?

The third part of this master thesis is to evaluate how deterministic dynamic programming (DDP) can be used for control management of the vehicle to increase the efficiency and minimise the consumed energy in a drive cycle. Therefore the following question is:

- Evaluate how DDP can be used to optimising a control sequence for a drive cycle to increase the efficiency and minimise the consumed energy?

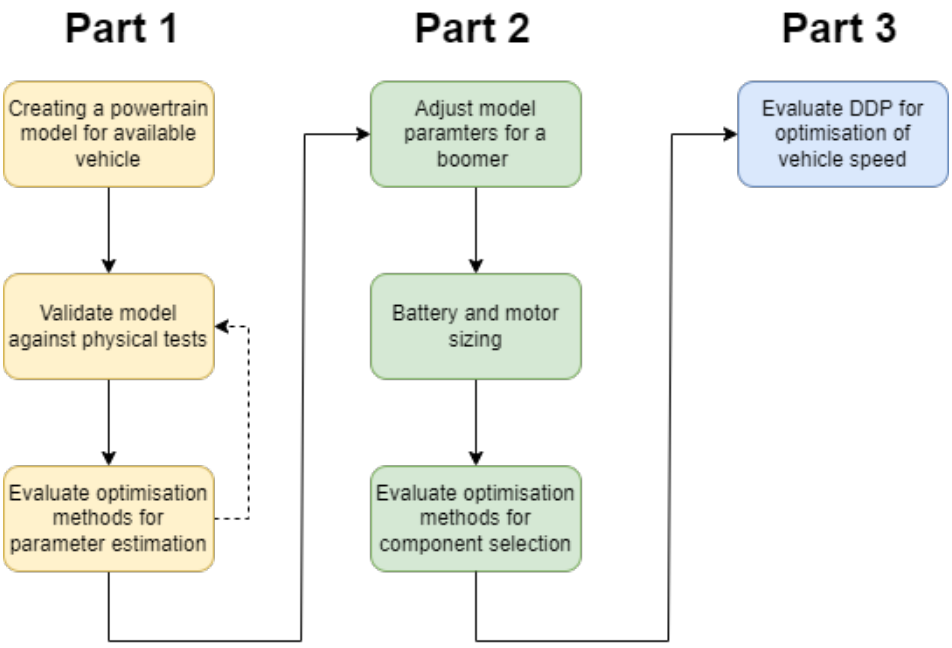

Figure 1.2: *Description of the thesis's three main parts.*

1.5 Delimitations

To be able to finish this thesis work in time, the following delimitations have been set:

- Since the focus of this thesis to create a model that provides the energy consumption from a drive cycle, components will not be modeled with more details than required for its purpose.
- Focus will not be on real-time control strategies such as PID controllers.
- Due to the unavailability of boomer for collecting measurement data the results will be validated against a available test vehicle of the same vehicle series.

2

Theory

In this chapter the theory required to create a vehicle model for energy consumption as well as the theory behind different optimisation methods will be introduced.

2.1 EV powertrain

There are different ways of configuring an Electric Vehicle (EV). A conventional electrical powertrain is used to explain the core components of a EV, shown in Figure 2.1. An electrical powertrain consists of both a mechanical and a electrical subsystem and where the theory of these components can be found in the different sections in this theory chapter. The electrical subsystem usually consists of electrical battery storage in section 2.3, electrical motor in section 2.4, and power electronics in section 2.5 while the mechanical subsystem consists of a transmission in section 2.6. A simple description of a electric powertrain can be seen in Figure 2.1 where T is torque, J is inertia, G is gear ratio, η is efficiency, ω is rotational speed, i is current, and V is vehicle speed [15].

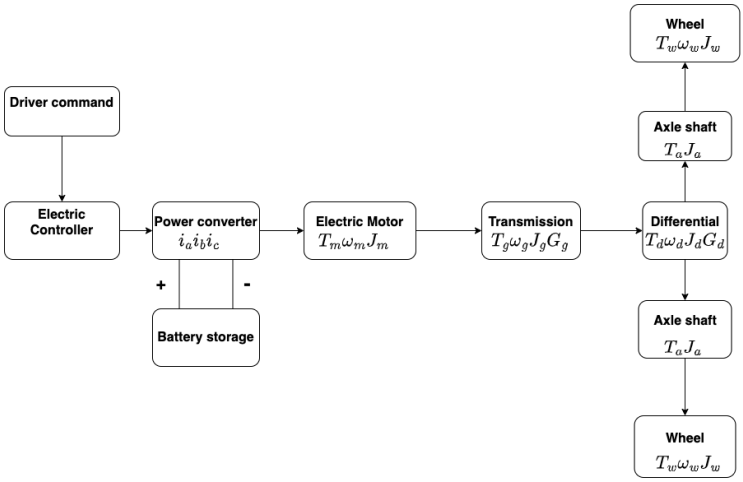

Figure 2.1: *Basic model of a electric powertrain [15].*

2.2 Modeling approaches

There are two primarily different approaches of predicting the energy consumption of a vehicle that is taken into account in this master thesis when modeling. These two approaches are Quasi-static (QSS) simulation and dynamic simulations. An overview of energy consumption for these modeling approaches is presented in Figure 2.2, where BT represent the battery, PB is the power converter, EM is the electrical motor, GB is the gear box, and V is the vehicle [8].

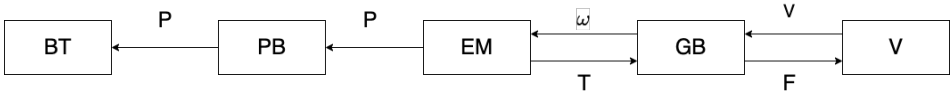

(a) *QSS modeling approach.*

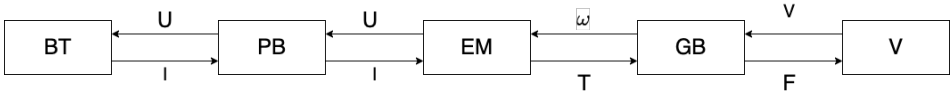

(b) *Dynamic modeling approach.*

Figure 2.2: *Two different ways for simulation modeling.*

2.2.1 Quasi-static approach

When using a QSS approach, the speed, acceleration and road slope are used as inputs to calculate the traction force. A drive cycle is used and is divided into small time steps where the velocity, slope angle, and accelerations are assumed

to be constant at each time step and the losses are calculated from the traction force using operating point dependant efficiencies to reduce the otherwise computationally heavy calculations in equation

$$F(t) = m_v \overline{a}_i + \frac{1}{2}\rho_a A_f c_d \overline{v}_i^2 + c_r m_v g cos(\overline{\alpha}_i) + m_v g sin(\overline{\alpha}_i) \tag{2.1}$$

where ρ_a is the air density, A_f is the front area of the vehicle, c_d is the air resistance,$\overline{v}$ is a constant velocity in a time interval, c_r is the rolling resistance, g is the gravitational force, m_v is the vehicle mass and $\overline{\alpha}$ is a constant slope angel in a time interval.

The QSS is usually good when minimising the fuel consumption in powertrains and it is possible to include driving patterns when using this approach but it is also a low computationally heavy approach. The problem with using this method is that it uses a backwards formulation and therefore physical causalities is not respected and the driving cycle needs to be known in prior and thus can not handle feedback or state events [8]. A QSS block diagram of a electrical powertrain is shown in Figure 2.2.

2.2.2 Dynamic Approach

The dynamic approach compared to a QSS approach is based on a dynamic description of the powertrain and is usually formulated with a group of ordinary differential equation (ODE). The dynamic effects in the powertrain can be described as

$$\frac{d}{dt}x(t) = f(x(t), u(t)), \qquad x(t) \in R^n, u \in R^m \tag{2.2}$$

where x is the state vector, u is the control signals and t is the time [8]. Comparing with the QSS approach, the dynamic approach demand input that as the request given to a physical machine and therefore a module that imitates the drivers behavior needs to be included. An example for this is that the motor requires a torque request that in turn is a result from a driver pressing the gas pedal. The problem with using a dynamic approach is that it is computationally heavy and thus is only recommended to be used when other options are not suitable [8]. An example of a dynamic approach block diagram of a electrical powertrain is shown in Figure 2.2.

2.2.3 Vehicle dynamic force model

To model a EV it is important to have a understanding of the dynamics of the model. A simple dynamic model can be seen in Figure 2.3 and the longitudinal vehicle dynamics is shown in the following equation:

$$m_v \frac{d}{dt}v(t) = F_t(t) - (F_a(t) + F_r(t) + F_g(t)) \tag{2.3}$$

where F_t is the traction force, F_a is the aerodynamic force, F_r is the rolling resistance and F_g is the impact of the gravitational force where these can be calculated with

$$F_a(t) = \frac{1}{2}\rho_a A_f c_d v^2, \qquad F_r(t) = c_r m_v g cos(\alpha), \qquad F_g(t) = m_v g sin(\alpha) \tag{2.4}$$

where ρ_a is the air density, A_f is the front area of the vehicle, c_d is the air resistance,v is the vehicle velocity, c_r is the rolling resistance, g is the gravitational force, m_v is the vehicle mass, and α is the slope angle.

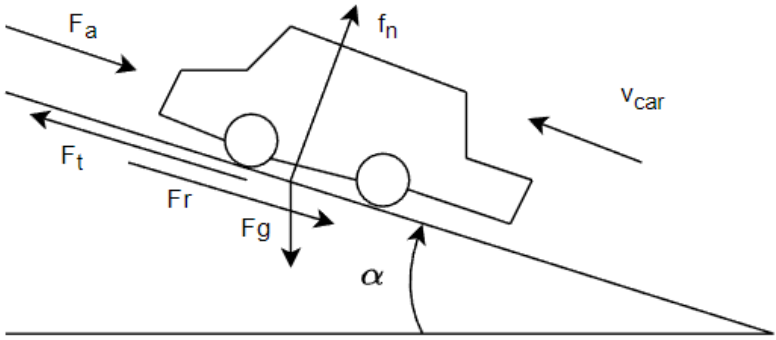

Figure 2.3: *Longitudinal vehicle dynamics.*

2.3 Battery

When modelling a battery using the QSS approach, the model in Figure 2.4 below is used. The variabel P_b is the required power, U_b is the battery terminal voltage, PA is the power electronics, I_b is the battery current that is an output from the PA, and BT is the battery. From this the charge or discharge is then calculated [8].

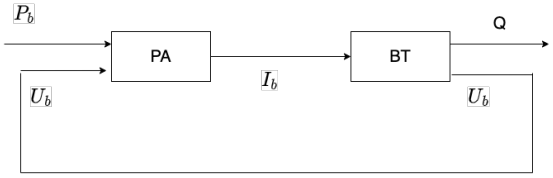

Figure 2.4: *QSS model of the battery where the system input P_b is battery power, and the output Q is the charge [8].*

To model the battery the current can be calculated using

$$I_b(t) = \frac{P_b(t)}{U_b(t)}, \tag{2.5}$$

where t is time, U_b is the terminal battery voltage and is a non-linear function of the state charge (SOC) and I_b as is described in equation (2.6).

$$U_b(t) = f(SOC(t), I_b(t)), \tag{2.6}$$

A simple model of the U_b can be modeled as

$$U_b(t) = U_{oc}(SOC) - R_{int} I_b, \tag{2.7}$$

where U_{oc} is the open circuit voltage and R_{int} is the internal battery resistance. The battery charge can be calculated as the integral of I_b over time as described in equation (2.8).

$$Q(t) = \int_0^t I_b(\tau)\, d\tau \tag{2.8}$$

The battery resistance $R_{battery}$ is calculated as

$$R_{battery} = f(U_b, SOC, T, t) \tag{2.9}$$

where f is a non-linear function and T is the battery temperature.

2.3.1 Battery discharge capacity

The battery capacity is not a set number but rather varies depending on the surrounding environment, such as the surrounding temperature. Therefore it is crucial to understand the behaviour of a battery to optimise the outcome and lower

the cost of transportation. Two of the parameters that heavily impact the battery discharge capacity are temperature and SOC [12]. The reason for this is that both temperature and SOC impacts the internal resistance of the battery and a increase of internal resistance results in higher losses when charging and discharging thus lowering the available capacity of the battery cell [6].

2.3.2 Battery temperature

The reason for the decrease in battery performance related to the power and energy capability is due to the fact that lower temperature affect the property of the electrolytes and increase their viscosity. This results in an increase of impedance of the directional migrations of the chemical ions and thus increases the internal resistance of the battery [11]. The total effect of different temperatures of a battery is shown below in Figure 2.5.

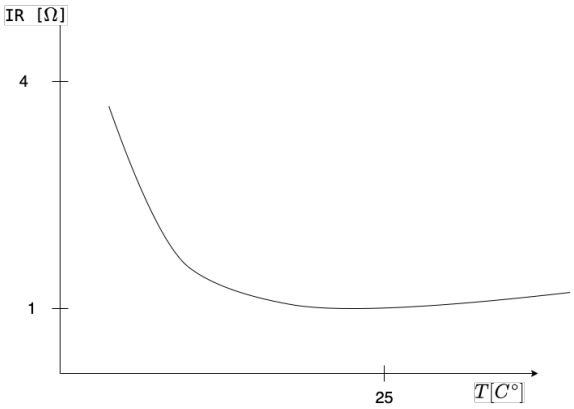

Figure 2.5: *Battery internal resistance dependency on battery temperature. The values in the graph are not actual values but instead arbitrary values to indicate the approximate impact of the internal resistance based on the battery temperature.*

2.3.3 Battery SOC

The battery state of charge is the percent of the total charge left in the battery divided with the initial charge in the battery, which represents the percentage of the total energy percentage left in the battery

$$SOC = \frac{Q_{initial} - Q(t)}{Q_{initial}} \tag{2.10}$$

where Q is the charge of the battery. The state of charge and the change in state of charge is dependent on different aspects [8].

The SOC impacts the performance of the battery since a low SOC increases the internal resistance of a battery, where the larges change happens between 0 and 30% in SOC [2]. Therefore a low SOC results in a high internal resistance and as stated before results in lower available battery capacity.

2.3.4 SOC-OCV graph

To model a battery storage in a accurate way, this is often done using a SOC vs. OCV curve which represent the thermodynamics and electronically process at different SOC. SOC stands for state of charge and is the percentage of the total battery energy that is currently available in the battery. OCV stands for open circuit voltage and is the electrical potential that is created when the terminals of a device is disconnected from a circuit. An example of a typical SOC-OCV function is seen in Figure 2.6 [20].

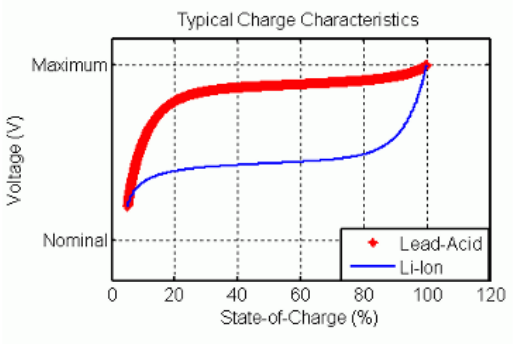

Figure 2.6: *Characteristics of a SOC-OCV curve obtained from standard Simulink library*

2.4 Electrical motor

In this section the theory for the electrical motor will be introduced and will include theory of the permanent magnet synchronous motor (PMSM) in section 2.4.1, the EV efficiency in section 2.4.2, and the calculations for motor requirements in section 2.4.3.

2.4.1 Permanent magnet synchronous motor

A PMSM is a type of synchronous motor were a synchronous motor consists of a rotor and a stator where the rotor is mounted on the axle driving the vehicle. The rotor in a PMSM motor is constructed using permanent magnets where the stator is constructed using armature wiring with a 3 phase current, thus creating a moving electrical field. This moving electrical field is then causing the rotor to rotate as the rotor poles always strive to orient towards the opposite pole in the

stator. This creates the rotational force that we receive from the electrical motor and is then used to rotate the wheels of the vehicle [3].

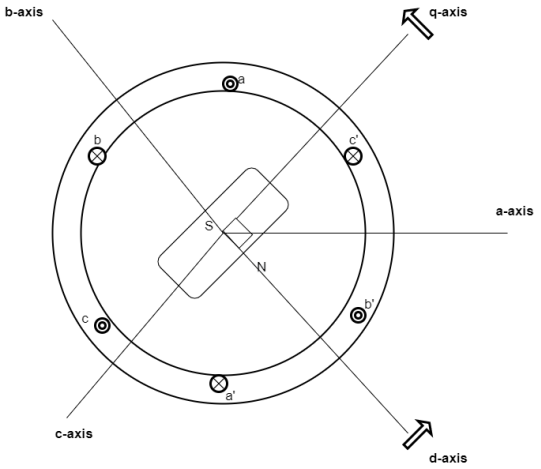

Figure 2.7: *Permanent magnet synchronous motor.*

The induced armature electromotive force, EMF, can be calculated as follow

$$e_a = E_m \sin(\omega t) \tag{2.11}$$

$$e_b = E_m \sin(\omega t - 120°) \tag{2.12}$$

$$e_c = E_m \sin(\omega t - 240°) \tag{2.13}$$

where E_m is the EMF amplitude, ω is the angular frequency. Since this a PMSM motor uses three phase current, the current is calculated as below

$$i_a = I_m \sin(\omega t - \theta) \tag{2.14}$$

$$i_b = I_m \sin(\omega t - 120° - \theta) \tag{2.15}$$

$$i_c = I_m \sin(\omega t - 240° - \theta) \tag{2.16}$$

where I_m is the current amplitude and θ is the difference between the EMF current. The electrical power can be calculated as

$$P_m = e_a i_a + e_b i_b + e_c i_c = \frac{3E_m I_m \cos(\theta)}{2} \tag{2.17}$$

The torque can be calculated as

$$T_m = \frac{P_m}{\omega_m} = \frac{3E_m I_m \cos(\theta)}{2\omega_m} \tag{2.18}$$

where ω_m is the mechanical motor rotational speed.

2.4.2 EV efficiency

To compensate for the efficiency in the motor, the input power from the motor need to be higher than the needed power to compensate for the losses in the motor. The most common way of dealing with motor efficiency is to use efficiency maps. The required electrical power, P_m needed to generate enough motor power or regenerated to the motor

$$P_m = \frac{T_m(t) \cdot \omega_m(t)}{\eta_m(T_m(t), \omega_m(t))^{\text{sign}(P_m)}}, \tag{2.19}$$

where η_m is a efficiency map for driving mode which has different efficiency for each operational point and each operation point is a combination of T_m which is the requested torque and ω_m which is the requested rotational speed. When driving in regenerative mode the motor efficiency map is often different and where η_g is the efficiency map for regenerative mode. In this case, the input to the QSS model of the electric motor is the required torque and rotational velocity and the output is the electrical power, this becomes the requested power from the battery as can be seen in Figure 2.2. If the power is positive then the electrical motor operates as a motor while if the power is negative it operates as a generator [8].

2.4.3 Motor requirements

When designing a motor there are some parameters that are important. To properly design a motor, the maximum rotational speed and maximum required torque is required. The required rotational speed is calculated as

$$\omega_{motor,max} = \frac{G_r v_{max}}{R_\omega} \tag{2.20}$$

where $\omega_{motor,max}$ is the maximal motor rotational speed, G_r represent the combined transmission ratio, v_{max} is the maximal vehicle speed, and R_ω is the wheel radius. The required torque can be calculated from

$$T_{motor,max,st} = \frac{R_\omega m_{v,loaded}}{G_r \eta_{gb} \eta_{motor}} g(\sin(\alpha) + f C_{stat} \cos(\alpha)) \tag{2.21}$$

where $T_{motor,max,st}$ is the maximal motor torque requirement for starting in a required slope, $m_{v,loaded}$ is the maximum vehicle mass, η_{gb} is the gear box efficiency, η_{motor} is the motor efficiency, g is the gravitational force, C_{stat} is the stiction coefficient, and α is the slope angle. The maximum power requirement is calculated as

$$P_{m,max} = \frac{m_v + 4\frac{J_\omega}{R_\omega^2} m_{v,loaded}}{2t_{req}} (v_{req}^2 + v_{m,base}^2) + \frac{2}{3} m_{veh} g f v_{req} + \frac{1}{5} *_d A v_{req}^3, \tag{2.22}$$

where f is the friction coefficient, C_{stat} is the stiction coefficient, ρ is the air density, c_d is the drag coefficient, t_{req} is the required time for going from one velocity

to another, v_{req} is the new speed requirement, $v_{m,base}$ is the current speed, A is the frontal vehicle area, and J_ω is the inertia. With certain needs for acceleration, it is possible to calculate the needed torque based on the required acceleration as

$$T_{motor,max,ac} = \frac{P_{motor,max}}{\omega_{motor,max}} \tag{2.23}$$

where $T_{motor,max,ac}$ is the maximum required torque from acceleration. This results in the maximum torque requirement from the motor explained in equation (2.24).

$$T_{motor,max} = max(T_{motor,max,ac}, T_{motor,max,st}) \tag{2.24}$$

2.5 Power converter

The power converter include both a DC-AC inverter as well as a DC-DC converter [15]. The inverter is controlling the speed and torque of the motor by inverting the DC voltage to three phase AC voltage which can be used by the electrical motor [8]. The inverter is the electrical controller used in the electrical powertrain and the efficiency of the electrical controller is assumed to a constant. The DC-DC converter is a elechtromechanical device that converts a DC source from one voltage level to another [14].

2.6 Transmission

In the transmission part of the theory, the transmission components included in the models created in this master thesis are explained. In this section the theory for the differential in section 2.6.1, the wheels in section 2.6.2, the gear box in section 2.6.3, torque converter in section 2.6.4, and the planetary gear in section 2.6.5 are explained.

2.6.1 Differential

A differential is a important part in a vehicle powertrain. It is used to control the wheel speed when turning by splitting the torque from the motor. This allows the left wheel to have a higher rotational speed than the right wheel when turning right [15]. The equation used to calculate the wheel torque is

$$T_{wheel,l} = T_{motor}/2, \qquad T_{wheel,r} = -T_{wheel,l} \tag{2.25}$$

where index r and l represent right and left wheel. The motor rotational speed is calculated as

$$\omega_{motor} = \frac{\omega_{wheel,l} + \omega_{wheel,r}}{2} \tag{2.26}$$

2.6.2 Wheels

To calculate the wheel inertia, J_{wheel} and the rotational energy, W_k the following equations are used

$$J_{wheel} = Cm_{wheel}r_{wheel}^2 \qquad W_k = \frac{J_{wheel}\omega_{wheel}^2}{2} \tag{2.27}$$

where C is a specific constant for every unique wheel and m_{wheel} is the mass of the wheels.

2.6.3 Gear box

A gear box transfers power from a combination of torque and rotational speed to another combination of torque and rotational speed. If the losses in a gear box is neglected then the gear box can be explained as

$$\omega_1 = \gamma\omega_2 \qquad T_2 = \gamma T_1 \tag{2.28}$$

where γ is the gear ratio, ω_i is the rotational speed, T_i is the torque, index i = 1 is for the shaft connected to the motor and index i = 2 is for the shaft connected to the wheels [8].

Gear box ratio

Deciding gear ratio is a complex problem but it is possible to set the limits of the gear ratio. The high and low gear ratio limits can be found using

$$\gamma_{high} = \frac{m_v g r_\omega \sin(\alpha_{max})}{T_{e,max}(\omega_e)}, \qquad \gamma_{low} = \frac{r_\omega c_{m,max}}{v_{max}} \tag{2.29}$$

where r_ω is the wheel radius, $c_{m,max}$ is the top continuous engine rotational speed, v_{max} is the maximum vehicle speed, and α_{max} is the largest possible road slope. The smallest gear usually work as either the gear to allow the vehicle to reach the maximum speed or to be the gear ratio that minimises the consumed energy and maximises the system efficiency. Therefore this gear can differ depending on what is the priority when choosing the gear ratio [8].

Gearbox efficiency

The efficiency of a gearbox depends on several factors. An approximation of the gear box efficiency can be calculating the input power to the output power. The equation for traction mode is

$$T_2\omega_\omega = \eta_{gb}T_1\omega_e - P_{0,gb}(\omega_e),\ T_e\omega_e > 0 \tag{2.30}$$

and the following for regenerative breaking mode

$$T_1\omega_e = \eta_{gb}T_2\omega_w - P_{1,gb}(\omega_e),\ T_e\omega_e < 0 \tag{2.31}$$

where $P_{0,gb}$ is the power required to idle at a certain rotational speed ω_e, and η_{gb} is the efficiency of the gear box. The efficiency of a gear cog-wheel gear box in cars are usually between 95 and 97 percent [8].

2.6.4 Torque converter

A torque converter is used when the rotational speed of the wheels and the motor is not similar and therefore needs to be disconnected, this is due to the fact that the impeller and turbine having the function to operate individually of each other. Instead of using a clutch, a torque converter can be used for this [8]. A torque converter consists of a impeller, also called the pump which drives the converter and is connected to the torque source and a turbine, which is the driven part and also the output of the torque converter. A torque converter can by simplicity be explained as two fans facing each other where if one fan rotates, liquid cause the other fan to rotate. The results in the motor and the wheels to be connected by a liquid and not mechanically connected resulting in the motor being able to rotate even if the wheels are fixed without resulting in mechanical failure in the axle between the wheel and the motor [10].

When the torque converter is not fully locked, the torque and the efficiency can be calculated as

$$T_{1,e}(t) = \xi(\phi(t))\rho_h d_p^5 \omega_2^2(t), \qquad T_{1,gb}(t) = \psi(\phi(t))T_{1,e}(t) \tag{2.32}$$

where $\phi(t) = \frac{\omega_{gb}(t)}{\omega_e(t)}$, d_p is the pump diameter, ξ is a gain function for the engine torque that depends on ϕ , ψ is a gain function for the gear box torque that depends on ϕ, and ρ_h is the density converter fluid.

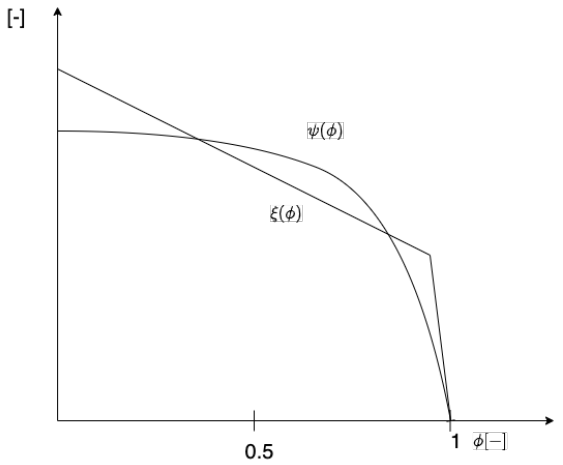

Figure 2.8: *The impact on omega ratio.*

The efficiency of the torque converter can be calculated as

$$\eta_{gb}(t) = \frac{\omega_{gb}(t)T_{1,gb}}{\omega_e(t)T_{1,e}} = \psi(\phi)\phi \tag{2.33}$$

Lock up clutch

A clutch compared to a torque converter does not have a torque ratio and therefore the impeller torque is equal to the turbine torque. The torque calculation can be seen in equation

$$T_{1,e}(t) = T_{1,gb}(t) = T_1(t), \tag{2.34}$$

where the only phase where clutches produce losses is the phase from where the clutch is activated until the impeller and turbine rotational speeds are equal. The Energy lost in this phase is calculated as

$$E_c = \frac{1}{2}\Theta_v \omega_{w,0}^2, \tag{2.35}$$

where Θ_v is the combined inertia on the parts after the torque converter and $\omega_{w,0}^2$ is the rotational speed where ω_e and ω_{gb} has the same rotational speed. The resulting torque during this phase is equal to

$$T_1(t) = T_{1,max}(\Delta\omega(t))u(t), 0 \leq u(t) \leq 1 \tag{2.36}$$

where the $\Delta\omega(t) = \omega_{1,e}$ - $\omega_{1,gb}$ and $u(t)$ is the actuation signal. A lockup clutch is used as it forces the impeller and turbine to be connected and therefore the turbine speed will rotate in relation to the impeller rotation which removes the slip and also the losses caused by the slip [8].

2.6.5 Planetary gear

A planetary gear consists of three different parts, a sun gear, planet gears and a ring gear, where the axle of all these gears are parallel with each other. A planetary gear consists of one or more outer gears, also called planet gears, these are revolving around a central gear, also called the sun gear. Planetary gears can be mounted in different ways but the planet gears are usually mounted on a carrier and rotates relative to the sun gear. The last part is the ring gear that is surrounding the planetary gears with internal toothing that meshes with the planet gears. These types of gear are good since they are simple and small in size [7].

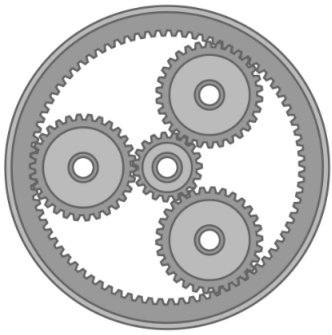

Figure 2.9: *A planetary gear where the inner gear is the sun gear, the outer ring is the ring gear and where the three cogs between the carrier and the sun gear are the planetary gears.*

Planetary gears are often used as they are one of the best ways for transporting power in high torque applications since they have better efficiency than more traditional gears resulting in an increase use of these gears in automotive applications. They are also a interesting choice due to the fact that they do not require as much space as traditional ones and that they are a high-power to weight option. Combining this with that planetary gear allows the driveshaft and the motor to be concentric to each other, the planetary gear box is a good choice to use together with hub motors.

2.7 Driveline configurations

In this section, the theory for the axle motor configuration in section 2.7.1 and hub motor configuration in section 2.7.2 are explained.

2.7.1 Axle motor

An axle motor is a motor that is placed on the wheel axles instead of a centralised position. The motor configuration can be seen in Figure 2.10, both motors uses the same battery although each of the axle motors have their inverter where controller 1 controls axle 1 which powers wheel 1 and wheel 4 and controller 2 controls axle motor 2 which powers wheel 2 and 3.

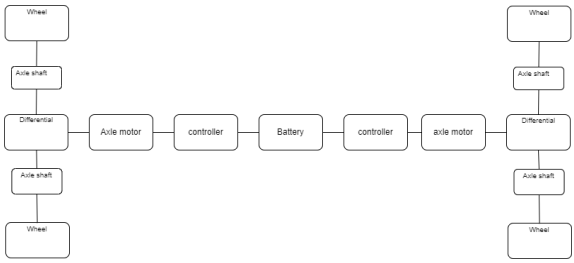

Figure 2.10: *Powertrain with axle motors.*

2.7.2 Hub motor

A hub motor is compared to a central motor connected to all wheels, a motor that is locally placed on each wheel as seen in Figure 2.11. This is called distributed drive transmission and has a shorter power transmission compared to a centralised drive since the direct coupling on the wheel removes all the mechanical parts such as the differential, gear box and possibly a torque converter. This results in the possibility to remove a lot of vehicle space but also lower the weight of the vehicle. Apart from this, removing components from the transmission results in lower efficiency losses in the transmission [19].

Another difference between hub motor and centralised motor, is that when having a centralised motor, often a high speed-low torque motor is used to increase power-weight ratio, this requiring a transmission and a gear box while hub motors usually use a low speed-high torque motor directly on the wheel. The centralised motor that is directly coupled with a gearbox and where the powertrain can be controlled in such a way that the motor always operates close to maximum efficiency. For a hub motor, it will instead operate in all the operating ranges, and therefore result in a lower efficiency, which is one of the disadvantages of this configuration.

Another impact of implementing a hub motor is that since the hub motor is mounted on the wheel it increases the mass of the wheel and therefore the wheel inertia. This results in a higher required power when accelerating the vehicle [19].

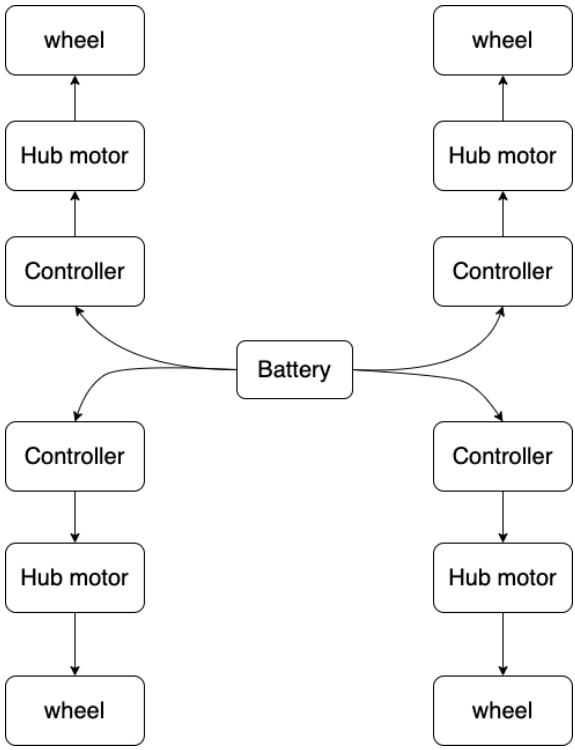

Figure 2.11: *Powertrain with hub motors.*

2.8 Sensitivity analysis

There are many parameters that impacts the required traction force to drive a vehicle. The ones that effect the traction force the most are $A_f c_d$,c_r and m_v. To find the relative impact of a parameter a sensitivity analysis can be conducted. This analysis can be done using

$$S_p = \lim_{\delta_p \to 0} \frac{\overline{[E_{p+\delta_p}} - \overline{E_p}]/\overline{E_p}}{\delta_p / p}, \tag{2.37}$$

where $\overline{E_p}$ is the average energy consumption from the drive cycle, p is the parameter value of where the sensitivity analysis is evaluated, δ_p is the change in the parameter value, and S_p will be compared between the different parameters chosen to be evaluated. The larger the value the more impact the parameter has on the energy consumption [8].

2.9 PID controller

A PID controller is a industrial control application that is used to regulate a output of a system. The PID function is conducted with a gain, a integral, and a derivative as described in

$$u(t) = K_p e(t) + K_i \int_0^t e(\tau)\, d\tau + K_d \frac{de(t)}{dt} \tag{2.38}$$

where $e(t)$ is the difference between the reference value and the measured value

$$e(t) = y_{ref} - y \tag{2.39}$$

where y_{ref} is the reference value, y is the measured value.

2.9.1 P-part

The P-part is multiplying with the error, having a too big gain might result in instability while having a too small gain can cause lag in the system. Therefore it is important to tune the gain value properly.

2.9.2 I-part

The I-part is proportional to the size of the error and the duration of the error and calculates the total sum of of the error over time. The effect implementing a integer is that it removes static errors between the reference and measured value.

2.9.3 D-part

The D-part is a derivative function that is results in a response proportional to the change rate in the signal therefore changes in the error will cause the controller to react faster and it is therefore important to tune this properly and to have a good filter to not react on noise.

2.10 Optimisation

Optimisation is a good tool to find an optimal design based on a set of prioritised criteria and limitation. Optimisation is used to mathematically find this optimum where it is very difficult for a human to understand what the optimum is. In this thesis optimisation will be used to identify parameter values to match a model to a physical machine as well as to be used to improve the use of the product. The optimisation methods that will be used in this master thesis is non-linear programming by quadratic lagrangian in section 2.10.1, genetic algorithm in section 2.10.2, and deterministic dynamic programming in section 2.10.3.

2.10.1 Non-linear programming by Quadratic Lagrangian

Non-linear programming by quadratic langrangian, is an implementation of a sequential quadratic programming (SQP) algorithm. This algorithm is one of the most successful method for solving constrained non-linearly optimisation problems for differentiable objective and constraint functions and is computationally efficient. The SQP algorithm is applied on non-linear optimisation problems (NLP) on the following form:

$$\begin{aligned} &\text{minimise} \quad f(x) \\ &\text{over x } \in \mathbb{R}^n \end{aligned} \tag{2.40}$$

$$\text{subject to} \quad h(x) = 0 \tag{2.41}$$

$$g(x) \leq 0, \tag{2.42}$$

where x is the state, f(x) is the objective functional, h(x) is the equality constraints and, g(x) is the inequality constraints [16].

For optimally x^* to be reached, the following necessary condition on the Lagrangian gradient need to be fulfilled

$$\nabla \mathcal{L}(x^*, \lambda^*, \mu^*) = \nabla f(x^*) + \nabla \lambda^T h(x^*) + \nabla \mu^T g(x^*) = 0 \tag{2.43}$$

where the vectors λ and μ refers to the Lagrangian multipliers.

SQP is an iterative process solving quadratic Programming (QP) subproblems repeatedly until the solution converges to a local minimum of the NLP. Since these QP subproblems in each iteration have to reflect the local properties of the NLP with respect to the current iterate x^k , following approximations on the NLP functions are made:

$$f(x) \approx f(x^k) + \nabla f(x^k)(x - x^k) + \frac{1}{2}(x - x^k)^T H f(x^k)(x - x^k) \tag{2.44}$$

$$g(x) \approx g(x^k) + \nabla g(x^k)(x - x^k) \tag{2.45}$$

$$h(x) \approx h(x^k) + \nabla g(x^k)(x - x^k) \tag{2.46}$$

and $Hf(x)$ refers to as the Hessian of the objective function, f [9]. Setting:

$$d(x) := x - x^k, \qquad B_k := Hf(x^k) \tag{2.47}$$

gives the following QP subproblem to be solved at each iteration:

$$\begin{aligned} &\text{minimise} \quad f(x^k) + \nabla f(x^k) d(x) + \tfrac{1}{2} d(x)^T B_k d(x) \\ &\text{over } d(x) \in \mathbb{R}^n \end{aligned} \tag{2.48}$$

$$\text{subject to} \quad h(x^k) + \nabla g(x^k) d(x) = 0 \tag{2.49}$$

$$g(x^k) + \nabla g(x^k) d(x) \leq 0 \tag{2.50}$$

The following properties can be set in the NLPQL solver in AMEsim:

- Relative gradient step
- Desired final accuracy, which is the termination accuracy to the Lagrangian gradient condiation described in equation (2.43)

2.10.2 Genetic algorithm

The genetic algorithm is a method for solving both constrained and unconstrained optimisations problems. This algorithm is a search heuristic and relies on a computer-based metaphor of Charles Darwin's theory of natural selection, inspired by the process that drives the biological evolution. The natural selection process relies on that the fittest individuals are selected for reproduction to later on produce offsprings of the next generation. In this algorithms, an individuals represents a set of parameter values [4][18]. This process can be divided into the following six parts which also are described in Figure 2.12:

- Initial population
- Calculate individuals
- Selection
- Reproduction
- Mutation
- Calculate individuals of mutation

The first step is about to randomly generate a population of individuals. Then this population are going through a fitness function that calculate how fit an individual is. In other words, it gives each individuals a fitness score, which describe their ability to compete with other individuals. These individuals are called "parents" and in the selection phase, parents with highest fitness score are selected to pass to the new generation. In the next phase, two randomly pairs of parents among the ones with higher score are selected in order to create new individuals with parameters close them. This new individuals are called "children" and replaces parents with lower fitness score. In the fifth part, some of the "children" are being mutated, which means their characteristics, i.e. parameters values are modified by adding small perturbations to their values in order to obtain diversity within the population and to prevent incomplete convergence. Then their fitness score is calculated and the whole process is repeated iteratively until the individuals converge to one or several best solutions, or until maximum set iterations are executed [4] [13].

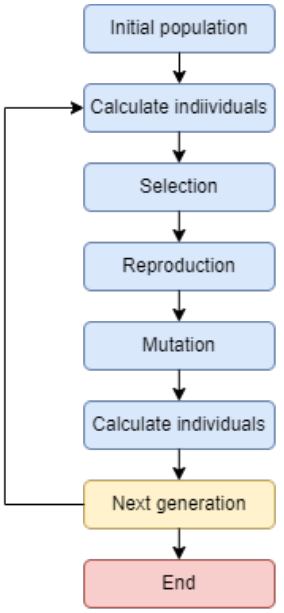

Figure 2.12: *Genetic algorithm process.*

An example of an application of the genetic algorithm is shown in Figure 2.13, where a gear ratio is optimised to minimise the energy consumption in a vehicle for a drive cycle, something that is be done in this thesis. Given a formulated optimisation problem, the first step is to randomly generate a set of gear ratios, within possible constraints. These gear ratios are called "parents" and are then going through a fitness function that will calculate their fitness score based on how they relate to the objective function, i.e, energy consumption. In the next step, gear ratios with highest score are selected to pass to the new generation. Among these parents, two randomly pairs of "parents" with higher score are selected to generate new gear ratios close to them, and these new gear ratios are called "children" and replaces "parents" with lower fitness score. In the next phase, some of the "children" are being mutated by adding small perturbations to the gear parameters. Then their fitness score is calculated and the whole process is repeated, but now with gear ratios one step closer to optimum. The process is repeated iteratively until the individuals converge to one or several best solutions, or until maximum set iterations are executed.

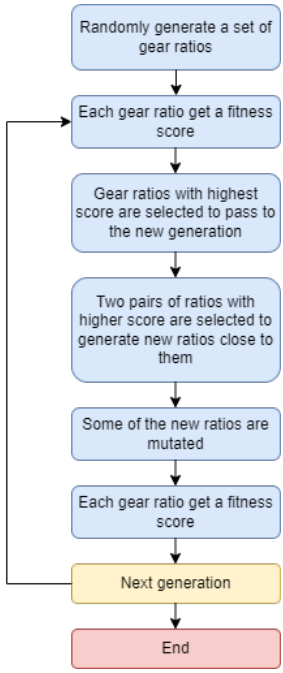

Figure 2.13: *Genetic algorithm applied to gear ratio optimisation.*

The following properties can be set in the genetic algorithm solver in AMEsim:

- Population size - number of individuals in the population.
- Reproduction ratio - percentage of "parents" replaced by "children" at each iteration.
- Max. number of generation - maximum number of iteration.
- Mutation probability - probability for each element of the population to have its discrete parameters mutated (i.e only used for discrete parameters).
- Mutation amplitude - amplitude of noise added to parameters, number between 0 and 1.
- Seed

The advantage of genetic algorithm is that it can solve complex multi objective optimisation problems and is searching for global optimum solution [17][18]. The disadvantage, however, is that the algorithm is computationally heavy and thus time consuming [5].

2.10.3 Optimal control

The vehicle used in this master thesis is a heavy duty vehicle where it is beneficial to optimise the vehicle speed to minimise the energy consumption.

Deterministic dynamic programming

Deterministic dynamic programming (DDP) is explained in [8] and is a way of solving a optimal control problem where it finds the optimal solution of a problem with the drawback that it can be computationally demanding since the complexity is linearly increasing in time and quadratic increasing with increasing states and control signals. The complexity T is as follows

$$T = kN_t N_x^2 N_y^2, \tag{2.51}$$

where k is the computational time for 1 computation, t is the time discretisized time vector and y and x are discretisized points in the grid. Dynamic programming problem formulation can be written as below where the objective is to minimise the performance function, i.e the total cost function $\mathcal{J}(u)$ as

$$\mathcal{J}(u) = \Theta(x(t_b), t_b) + \int_{t_a}^{t_b} L(x(t), u(t), t)dt, \tag{2.52}$$

where t_a corresponds to the first time state and t_b the second last time state. Thus, $\Theta(x(t_b), t_b)$ is the cost from t_b to the last time state t_N i.e., the last time step. The remaining total cost is given by $\int_{t_a}^{t_b} L(x(t), u(t), t)dt$. The system model constraints is

$$\frac{d}{dt}x = f(x(t), u(t), t), \qquad x(t_a) = x_a, \tag{2.53}$$

where the control signal constraints are

$$u_k \in U_k \qquad \text{and} \qquad x_k \in X_k \tag{2.54}$$

$x(t)$ and $u(t)$ are discretisised and are the functions on the time interval $t \in [t_a, t_b]$. The idea is to find the optimal control sequence for

$$\pi^0(x_0) = \{u_0, u_1, ..., u_{N-1}\}, \tag{2.55}$$

The Bellman theory and algorithm is used in this case and is starting at the end where $t = N$ and proceeds back in time to $t = 0$. During this it conducts the best cost-to-go function and stores the control signals. The algorithm used for solving this graph problem is shown in Figure 2.14.

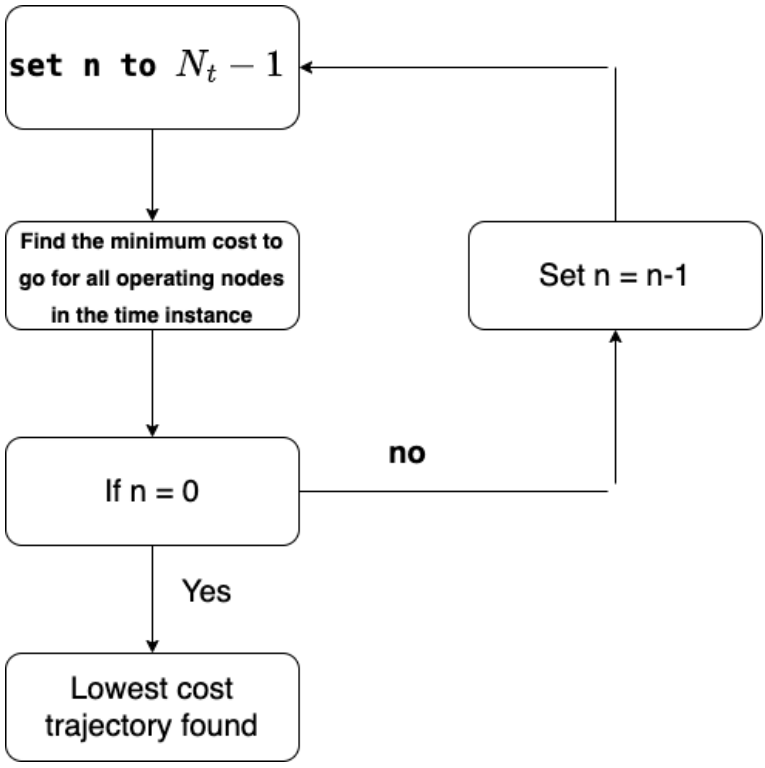

Figure 2.14: *The DDP algorithm.*

A walk thought of the algorithm is shown below where the transitioning cost in operating node 4 and from t_{N-1} to t_N where the control signal with the lowest cost-to-go is saved and associated with node 4 and time t_{N-1}. This can be seen in Figure 2.15 and 2.16 where the procedure is done for each of the 4 nodes where the result can be seen in Figure 2.17 where all nodes in that time instance has been associated with a lowest cost and a control signal. The same process is then implemented in all of the discretisized time steps and the optimal node trajectory can be found from the trajectory with the lowest starting cost. This can be seen in Figure 2.18 where the optimal path is marked with red and the result is the green trajectory.

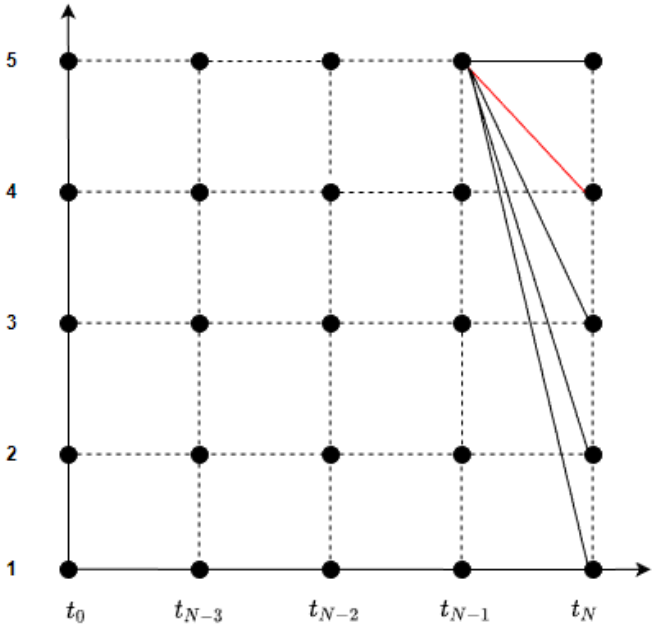

Figure 2.15: *The transitioning cost from node 5 to the all the other nodes in the given time instance is evaluated and the one with the lowest cost to go is chosen and marked with red.*

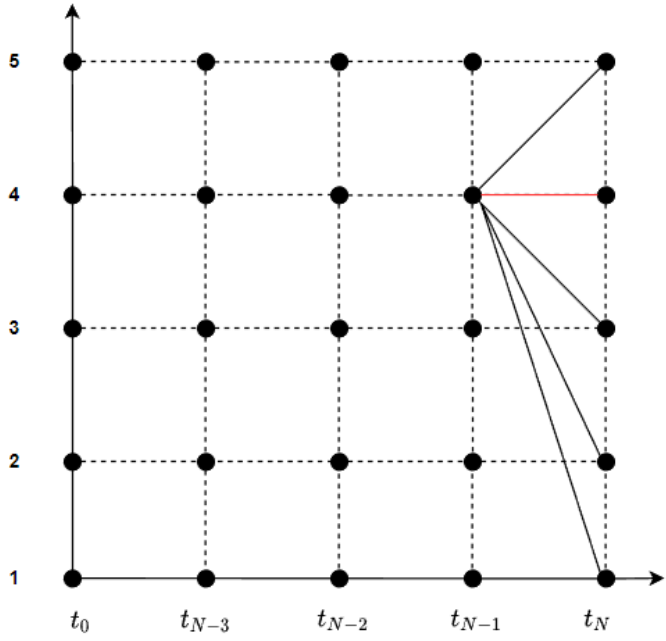

Figure 2.16: *The transitioning cost from node 4 to the all the other nodes in the given time instance is evaluated and the one with the lowest cost to go is chosen and marked with red.*

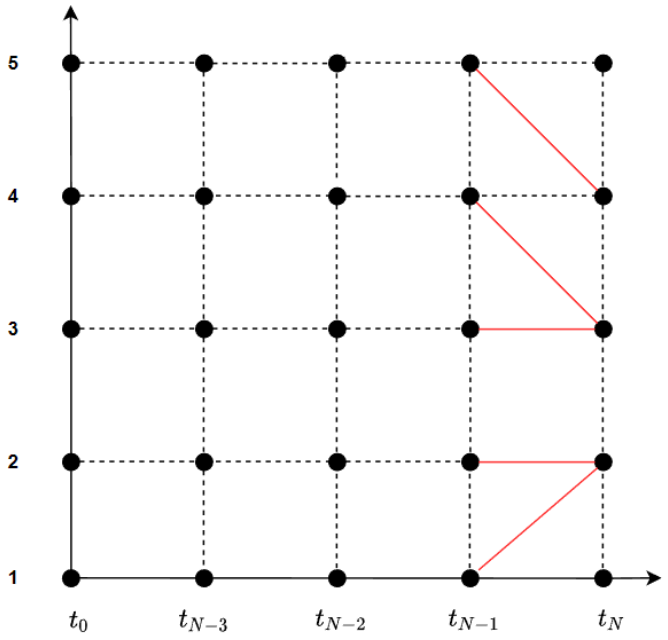

Figure 2.17: *The results from evaluating all the nodes at time t_{N-1} and the nodes are associated with the lowest cost to go.*

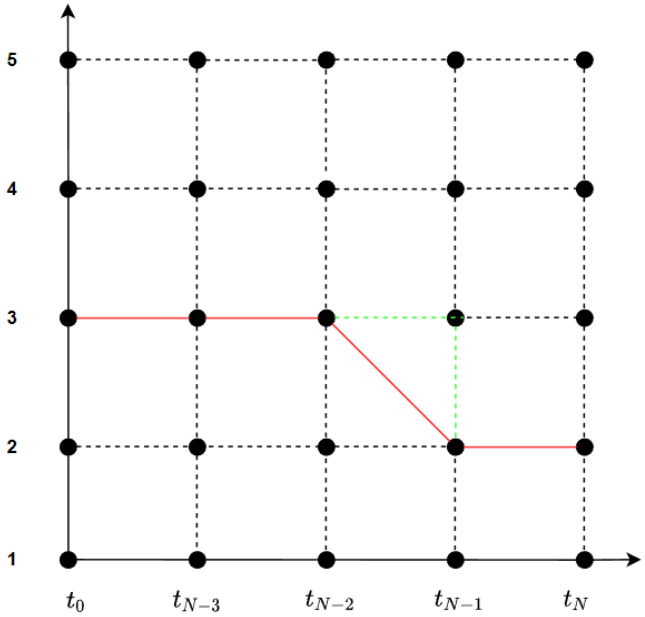

Figure 2.18: *The optimal control trajectory is shown where the red line is the optimal path and the green line is the interpretation of the solution where node 2 is active both between t_0 and t_{N-3} and between t_{N-2} and t_{N-1} and node 3 is active between both t_{N-3} and t_{N-2} and between t_{N-1} and t_N.*

3
Method

The expected outcome of this master thesis is to evaluate the efficiency for different configurations of electrical powertrains at Epiroc. To do this, the base model of the powertrain will be created and then with that as a base, the different configurations will be created and the different efficiencies will be calculated. Different methods will also be presented to be used by Epiroc that with the use of different optimisation algorithms, both to match the AMEsim model with the physical model and to optimize choice of components and the use of the physical model.

3.1 Quasi-static or dynamic approach

The first thing to be decided is whether to use a quasi-static approach or a dynamic simulation approach explained in section 2.2. Since the driving cycle is known in prior, see Figure 3.4, it is possible to use both of these approaches. Both of these have their advantages and disadvantages, where QSS is generally preferred due to its low demands on computational power, while the dynamic approach takes the dynamic behaviors into account, which is also important since it increases the model's accuracy and reliability. Since this thesis focuses on both meeting the drive cycle's criteria and the driveline's efficiency, it is important to include the dynamic approach to the driveline parts that affect these two, otherwise QSS is preferred. Therefore, a combination of these two approaches should be considered.

3.2 Model of the available test vehicle

Before creating a AMEsim model to be used for the boomer, a model for a available test vehicle was modeled as explained in section 2.1. The reason for this is since Epiroc had a machine available in the workshop that can be used as a validation for the AMEsim model. This validated AMEsim model and its parameters can then be scaled to match the boomer. The AMEsim model of the available test vehicle is shown in Figure 3.1.

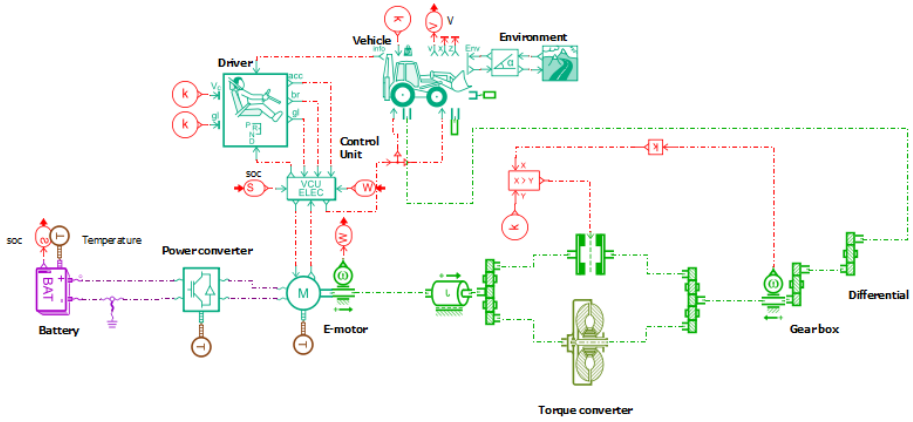

Figure 3.1: *Model of the available test vehicle.*

3.2.1 Vehicle model

The powertrain of the available test vehicle consists of a battery, electrical PMSM motor, a electrical controller (power converter), a gear box, a torque converter with a lockup clutch and, a differential and wheels.

3.2.2 Vehicle weight

The weight of the machine is different for the different setups and each of the different setups was created by mapping what parts will make a huge weight difference between the current diesel driven vehicle compared to the different electrical motor configurations and then create a base weight of what is common for all of the options and add the components needed for the different options.

3.2.3 Vehicle driver

The vehicle driver is implemented in AMEsim from the AMEsim library where the vehicle driver is included to represent an actual driver and takes the drive cycle and environment as input and output a torque.

3.2.4 Vehicle controller

The vehicle controller was created using a vehicle controller unit, VCU block in AMEsim which is a normal PI controller considering the SOC, acceleration command from driver, breaking command from driver, motor rotational speed, electric motor characteristics and then provides a motor torque command and a vehicle breaking command. It uses a PI controller where the gains was tuned to create a model that matched the measured data from the physical model. This PI controller is tuned to follow a given drive cycle.

3.2.5 Battery

The battery created was used by implementing a battery pack existing in AMEsim where the battery parameters such as OCV curve, internal resistance etc. was implemented.

3.2.6 Electrical motor

The electrical motor was built in a similar way as with the battery where a standard motor was chosen from AMEsim library where the motor then was created by implementing motor parameters such as continues and maximum torque, power and speed characteristics and where based on that, AMEsim created a matching efficiency map.

3.2.7 Electrical controller

The electrical controller was implemented as a component from AMEsim library that represent an inverter where the efficiency of the controller is implemented.

3.2.8 Torque converter with a lockup clutch

The torque converter was created by picking a torque converter from AMEsim library and where the torque ratio and the speed ratio was implemented based on values received from the data sheet of the torque converter. A clutch was also implemented in parallel of the torque converter with a control signal as a input controls the clutch. This way the clutch is acting as a lockup-clutch that is used in a torque converter.

3.2.9 Gear box and planetary gear

In this thesis both a regular gear box and a planetary gear is used. Although based on limited technical information of the components and that the function of the components for this thesis is to provide a efficiency and a gear ratio, a simple gear reducer, which has the same function as a gear box but where specific mechanical details are not needed in the model, is used since a reducer provides the functions needed in this master thesis.

3.2.10 Estimated parameters

When creating a model of a available test vehicle, some of the parameters are hard to measure or difficult to calculate and therefore needs to be estimated. Instead of estimating these parameters with trial and error, these parameters are identified using optimisation methods, which will be described in section 2.6.2.

3.3 Validate the model on available test vehicle

The validation of the available test vehicle is done first individually for the motor as well as the battery while the transmission from the motor to the wheel is evaluated in total since there is not enough data to validate each of these components individually. These parameters are validated based on data received from test cycles at Epiroc.

3.3.1 Battery validation

The battery was validated by using the test data from Epiroc and by using the collected battery temperature and current where the battery voltage and state of charge was evaluated and validated against another and the AMEsim model for the validation is seen in Figure 3.2.

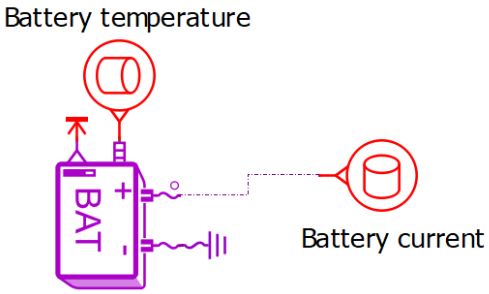

Figure 3.2: *AMEsim model for battery validation.*

3.3.2 Transmission - parameter estimation and validation

Since it is very difficult and expensive to measure torque throughout a drive line, there is no available data of the measured torque and therefore validating the efficiency in the transmission is not possible. Although the data received from the test contains the rotational speed along the transmission and therefore this can be used to validate the dynamics of the transmission and parameters will be validated and modified to match the physical machine. To identify these unknown parameters, wheel speed and motor torque are implemented as inputs to the transmission model to obtain a simulated transmission input speed that can

be compared to measured data. The unknown parameters will be estimated with the use of different optimisation methods to match the measured data and will be explained in section 3.9.1. These unknown parameters are transmission inertia and friction losses, in particular coulomb friction and coefficient of viscous friction.

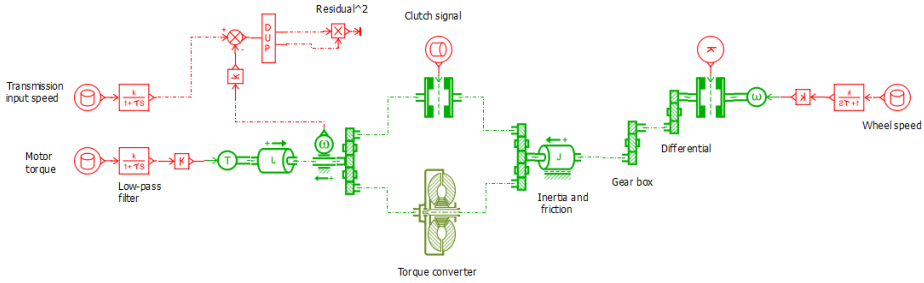

Figure 3.3: *AMEsim model used to validate the transmission part.*

3.4 Designing the powertrain for the boomer

The model of the powertrain is created based on the model of the available test vehicle where the model parameters are modified to match the boomer as well as two adjusted versions, one for the axle motor configuration and one for the hub motor configuration. Before the method is used, the base model needs to be created, this model is created based on a typical drive cycle for the boomer. This drive cycle consists of an interval of 8 minutes of velocity speed at 5 km/h with a 14 percent slope followed by a 1 minute rest. It is repeated for 45 minutes and can be seen in Figure 3.4.

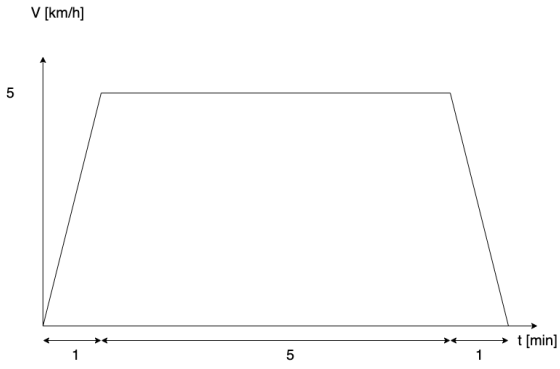

Figure 3.4: *The first cycle in the typical total drive cycle for the boomer.*

3.4.1 Parameter scaling

For some parameters, a correct value is hard to obtain and therefore these parameters needs to be identified based on measured data, obtained from the available test vehicle and then scaled to match the boomer. For the different vehicles, the friction parameters are assumed to be the same in this thesis while the inertia is to be scaled. For the inertia this is done by using the same constant C calculated for the available test vehicle from equation (2.27) but now using the parameters from the boomer as can be seen as

$$C = \frac{J_{wheel}}{m_{wheel} r_{wheel}^2} \tag{3.1}$$

3.4.2 Battery sizing

The battery is sized before the motor since the battery have an impact on how much current and energy can be delivered to the motor, but also an impact on the weight of the vehicle and therefore has an effect on the torque needed to follow the drive cycle. When sizing the battery, it is important to consider that the operational point of the battery is between 95 and 20 percent SOC due to a SOC lower than 20 results in a lower available battery capacity from the increase in internal resistance explained in section 2.3. The energy needed for one cycle is obtained from simulation of a drive cycle. To compensate for a more realistic battery with power losses, a constant at approximately 10 kWh is added from the calculated battery capacity to compensate for this.

3.5 Cooling motor and battery

The temperature of the battery and motor effect the performance of the battery and motor. Since the cooling system does not effect the efficiency of the powertrain apart from the actual temperature that the battery and motor is kept at. Due to the degradation of battery performance at both high and low temperatures explained in section 2.3.1, it is optimal to keep the temperatures between 26 and 29 degrees. This was from a conversation with our supervisor at Epiroc that led to the conclusion to the optimal temperature ranges for battery and motor seen in Table 3.1.

Component	Range	Unit
Battery	26-29	[°C]
Motor	20-60	[°C]

Table 3.1: *Optimal temperature range.*

Since objective in this thesis is to evaluate the powertrain efficiency, when testing the efficiency for the different configurations, the motor and battery temperature will be kept constant. The reason for this is that no cooling system is

implemented and that at the same temperature for all tests and where the cooling losses are included in the 10 kWh added battery capacity requirement.

3.5.1 Battery selection

Based on the battery requirements from the battery sizing a battery is chosen. Epiroc offer battery subpacks where the vehicle is equipped with an integer number of these battery subpacks where the integer number of batteries is chosen to have sufficient charge for the drive cycle.

3.6 Model for hub motor configuration

Introducing hub motors instead of the conventional centralised motor is done with the goal to compare the efficiency of the powertrain between hub motor and centralised. The model is implemented in AMEsim and consist of four smaller motors as described in section 2.7.2. Two of the motors are connected by a torque connector to the rear wheels and two are merged with a torque connector and implemented to the front wheels. There are two versions of this implementation where one consist of only the hub motors while the other is adding a planetary gear box in the hub motor. Due to changes in components, the total mass of the vehicle is changed and adapted in the AMEsim model.

3.6.1 Hub motor without planetary gear

In this case no planetary gear is implemented and thus requires motors to handle higher torque but a lower rotational speed, so called high torque-low speed motors. This is since there is no gear box that reduces the required torque from the motor or increases the required rotational speed. Since a hub motor does not have a gear box, a axle or a differential, these components are removed from the model to better match the effect of implementing a hub motor.

3.6.2 Hub motor with planetary gear

In this case a planetary gear box is implemented in each of the wheels to lower the required torque at each motor. This results in a similar weight as without the planetary gear but now a additional planetary gear will be added to each wheel.

3.7 Model for axle motors configuration

The axle motor is implemented before the differential and therefore will still have a gear ratio. The implementation is done in a similar way as with the centralised motor with a central battery but instead of providing energy to one motor it now provide energy to two motors where both of these motors are connected to a gear

box, this gearbox is used to illustrate the differentials, and then connected to the front and back vehicle axle. When using axle motors, the gear box is removed from the model.

3.8 Sensitivity analysis of the model

A sensitivity analysis is explained in section 2.8 is done since one of the objectives of this master thesis is to analyze the impact of how different configurations impact the efficiency and the energy consumption of the vehicle. Different configurations impact the vehicle in different ways and therefore this analysis is done to understand how different changes in different parameters impact the energy consumption to easier understand where to focus to reduce the energy consumption but to use to understand what to focus on when creating the DDP vehicle model.

3.8.1 Mass sensitivity

Since the different configurations of motors heavily changes the weight of the vehicle, the vehicle mass is interesting to include in the sensitivity analysis. Examples of this is since different configurations changes the required motor sizes, the number of motors as well as the existence of mechanical powertrain components.

3.8.2 Front area sensitivity

Even thought the scope of the master thesis does not consider changes of frontal area, this usually has a big impact on the energy consumption and will be used as a reference to the mass of the vehicle.

3.8.3 Rolling resistance sensitivity

Even thought the scope of the master thesis does not consider changes of rolling resistance apart from the impact of the weight of the car has on the rolling resistance, this usually has a big impact on the energy consumption and will be used as a reference to the mass of the vehicle.

3.8.4 Wheel inertia sensitivity

Since one of the motor configurations results in a motor being placed in the wheel, this increases the mass of the wheel and therefore impacts the wheel inertia as well, therefore the wheel inertia is investigated.

3.9 Optimisation

In this thesis different methods will be introduced to use by Epiroc both to match the AMEsim model with the physical model as well as chose components and optimize the use of the physical machine.

3.9.1 Estimating parameters and optimizing components

A part of the thesis is to create a method to optimize the model both to create a model that better match the physical model but also that can be used to chose components to reduce the energy consumption of the vehicle.

Method to estimating parameters and optimizing components

This method can be used by Epiroc to optimize and chose components to minimise the energy consumption or other values that is desired to minimise or maximise or to better match the model to a physical model.

1. Set restrictions for gear ratio or other parameters that shall be optimised.
2. Create a objective function based on the requirements.
3. Set parameter limitations.
4. Choose optimisation model based on complexity of the problem.
5. Run optimisation.

Estimating the transmission inertia and friction

The estimation for the transmission inertia as well as the transmission friction was done using two different optimisation algorithms, the NLPQL algorithm explained in section 2.10.1 and the genetic algorithm explained in section 2.10.2. Both the genetic algorithm and the NLQPL optimisation used for estimation the inertia and friction are using the same problem formulation, to estimate these parameters, the objective function used is equation (3.7) and the limitations are set as seen in equation (3.4) to (3.6)

$$\begin{array}{ll} minimise & f(x) = \left(\omega_{in,measured}(t) - \omega_{in,simulated}(t)\right)^2 \\ overx \in \mathbb{R}^n & \end{array} \tag{3.2}$$

where the objective is to minimise the square of the differences between the measured and simulated rotational speed, by estimating the optimal transmission inertia, coulomb friction, and coefficient of viscous friction as mentioned in section 3.3.2. The simulated input speed is calculated using measured wheel speed and transmission ratios according to equation (3.3).

$$\omega_{in,simulated}(t) = \omega_{wheel,measured}(t)\gamma_{axle}\gamma_{gb} \tag{3.3}$$

In order not to investigate unreasonable values, constraints on each parameter that is estimated have been set to arbitrary values, which are formulated in equations (3.4) to (3.6). In these equations $T_{in,coulomb,fric,min}$ corresponds to coulomb friction and ν to coefficient of viscous friction.

$$J_{min} \leq J \leq J_{max} \tag{3.4}$$

$$T_{in,coulomb,fric,min} \leq T_{in,mcoulomb,fric} \leq T_{in,coulomb,fric,max} \tag{3.5}$$

$$\nu_{min} \leq \nu \leq \nu_{max} \tag{3.6}$$

Optimising the gear ratio using NLPQL algorithm

Since the axle motor configurations do not include any gear, component optimisation using NLPQL explained in section 2.10.1 can only be implemented to optimize the gear box ratio in the centralised motor configuration and planetary gear ratio in the hub motor configuration. The optimisation problem can be formulated according to:

$$\begin{aligned} &minimise \quad f(x) = \alpha_{energy} \int_{t_0}^{t_k} P_{consumed}\, dt + \alpha_{efficiency} \int_{t_0}^{t_k} \frac{1}{\eta_{motor}} dt \\ &over x \in \mathbb{R}^n \end{aligned} \tag{3.7}$$

where the total objective is to minimise the energy consumption and optimise the motor efficiency over a drive cycle. The energy consumption is obtained by integrating the power consumed $P_{consumed}$ while the motor efficiency η_{motor} is optimised by minimising $\frac{1}{\eta_{motor}}$. To weight each objective in the total objective functions, penalty parameter α is used. To keep optimisation values within the physical limits of the vehicle, constraints have been implemented and are presented in equations (3.8) to (3.16).

$$SOC \leq SOC_{max} \tag{3.8}$$

$$-SOC \leq -SOC_{min} \tag{3.9}$$

$$V_{battery,cell} \leq V_{battery,cell,max} \tag{3.10}$$

$$-V_{battery,cell} \leq -V_{battery,cell,min} \tag{3.11}$$

$$I_{battery,cell} \leq I_{battery,cell,max} \tag{3.12}$$

$$-I_{battery,cell} \leq -I_{battery,cell,min} \tag{3.13}$$

$$T_{motor} \leq T_{motor,max} \tag{3.14}$$

$$P_{motor} \leq P_{motor,max} \tag{3.15}$$

$$\omega_{motor} \leq \omega_{motor,max} \tag{3.16}$$

3.10 Vehicle speed trajectory optimisation using deterministic dynamic programming

In this method section, the method for optimizing the speed using a DDP will be explained.

3.10.1 Method to optimize the vehicle speed using DDP

Using DDP to optimize the vehicle speed is a good way of optimising the vehicle speed in a drive cycle. The DDP that was created can easily be used by Epiroc for future use for their different vehicle, both for vehicle with a driver as well as for self driving cars. The DDP can be modified to optimize not only the vehicle speed and where a simple method to use the script is described below.

1. Optimize the AMEsim model.
2. Implement changes to the script based on the requirements.
3. Run script.
4. Export result optimised trajectory to AMEsim.

The speed trajectory optimisation was done using Matlab where the parameter values in Matlab are imported from AMEsim before each optimisation. Therefore the vehicle parameters can be optimised in AMEsim and the optimisation done in Matlab.
The reason for using DDP is because it gives a optimal velocity trajectory from the entire drive cycle where it is not needed to divide the drive cycle into sections as with NLPQL. Therefore it is powerful when the slope variation is more varying as well when the global optimum is required. Althought since only the global optimum is obtained, local optimum that might be almost as low in energy but faster might be missed.

3.10.2 Boomer model in Matlab

The model was created in Matlab where this model was approximated and simplified QSS model weas be used. The model approximation used is based on the sensitivity analysis where it can be seen that the mass has the biggest impact on the energy consumption and therefore the model will be based on this which results in the vehicle torque equation as below

$$T_{wheel} = r_w * (F_r + F_g) = r_w m_v g(c_r v cos(\alpha) + sin(\alpha))$$

and the electrical motor power is calculated as

$$P_{electrical} = \frac{T_{wheel}\gamma_{tot}}{\eta_{gb}\eta_{motor}} \frac{\omega_w}{\gamma_{tot}}$$

where ω_w is the wheel rotational speed calculated as

$$\omega_w = \frac{v}{r_w}$$

3.10.3 Objective function

The objective function used in the DDP is created to minimise the consumed energy but is also including a penalty for high acceleration as well as low vehicle speed. The function used is shown below

$$J_k(x_k) = \int_{t_a}^{t_b} P_{electrical} + \int_{t_a}^{t_b} \frac{\alpha_{penalty,v}}{3.6v}\, dt + \int_{t_a}^{t_b} \alpha_{penalty,a}(v - v_{opt})^2\, dt$$

where $\alpha_{penalty,v}$ is a penalty factor for vehicle speed, and $\alpha_{penalty,a}$ for vehicle acceleration.

3.10.4 Calculating the limits

These limits are calculated based on the physical limits on the motor and will vary over time, depending on the state of the vehicle.

Acceleration limit

$$a_{max} = (F_{max,wheel} - (F_s + F_r + F_a))/m_v$$

Speed limit

$$v_{max} = \frac{P_w R_w}{T_w}$$

Torque

$$T_{motor,min} \leq T_{motor} \leq T_{motor,max} \tag{3.17}$$

Power

$$P_{motor,min} \leq P_{motor} \leq P_{motor,max} \tag{3.18}$$

Rotational speed

$$\omega_{motor,min} \leq \omega_{motor} \leq \omega_{motor,max} \tag{3.19}$$

3.10.5 Penalty factors

The penalty factors are implemented to create a penalty on the behaviours that are not wanted and and are approximate values based on how much impact is wanted from these penalties. These penalty factors are parameters that weight the different objectives in the objective function and are tenable parameters. The penalties that are included in the DDP are, acceleration penalty, penalty for slow driving as well as penalty for high energy consumption.

3.11 Assumptions set within the scope of this master thesis

When creating this model the aim is to use it to evaluate the efficiency of the powertrain, this results in assumptions of for example that subsystems supporting the power that does not ad any value to the main purpose of this master thesis. Some assumptions made throughout the thesis are listed below.

- The cooling system cooling the battery and motor effectively keep the motor and battery within optimal operating temperature.
- Constant efficiencies in gearbox and differential.

4

Results

In this chapter the results received in this thesis are presented. Most of the graphs in this section will be normalised to avoid showing sensitive material. In this chapter the results of the model for the available test vehicle in section 4.1, estimation of powertrain inertia and friction in section 4.2, model of the centralised motor in section 4.3.1, model of the axle motor in section 4.3.2, model of the hub motor in section 4.3.3, optimisation of the gear ratio in section 4.5.1, and velocity trajectory optimisation in section 4.6.1.

4.1 Model of the available test vehicle

This section covers the modelling results of the available test vehicle, including the final AMEsim model and model validations.

4.1.1 AMEsim model

The result of the AMEsim model for the available test vehicle is based the EV vehicle modeling explained in section (2.1) and is shown in Figure 4.1.

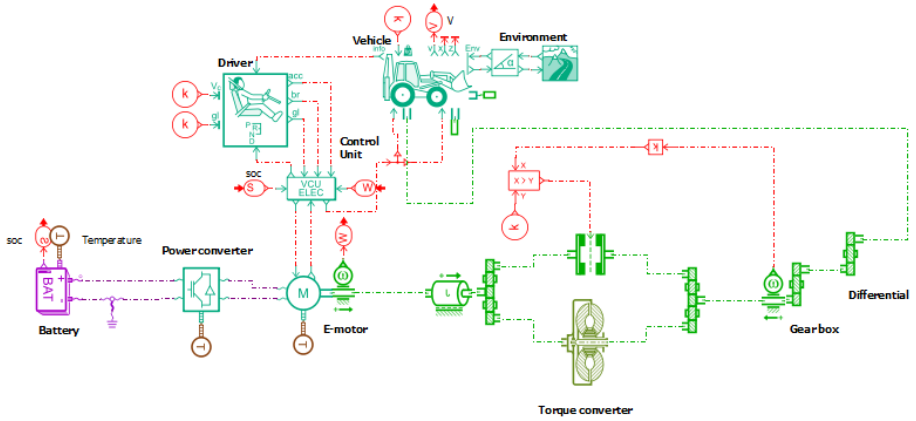

Figure 4.1: *AMEsim model of the centralised motor configuration.*

4.1.2 Validation

The validation of the avaiable test vehicle was done on several parts of the powertrain. The validation was conducted by a physical test drive cycle where the vehicle component validation and parameter estimation was conducted by implementing measured data into the model and compare the results with measured data. The result from the validation and parameter estimation is shown in this section.

Battery validation

The battery validation was conducted as in section 3.3.1 and after implementing the battery data into the AMEsim model the normalised collected data and the simulated data, which is adapted to the normalised measured data are shown in Figure 4.2. The residual of these plots are shown in Figure 4.3 where it can be seen that the simulated voltage is slightly higher than the collected data of the voltage. Although the difference between the data and the simulated voltage is at largest 6 % which is close. The difference that occurs is believed to be because of that the simulation bases its calculations on a completely new battery while while measured data is collected from an older and used battery i.e, one that has aged. It can also be seen that the measured voltage drops faster than the simulated voltage at the end of the drive cycle, this is probably because of aging from the test battery or based on a small difference in the OCV curve.

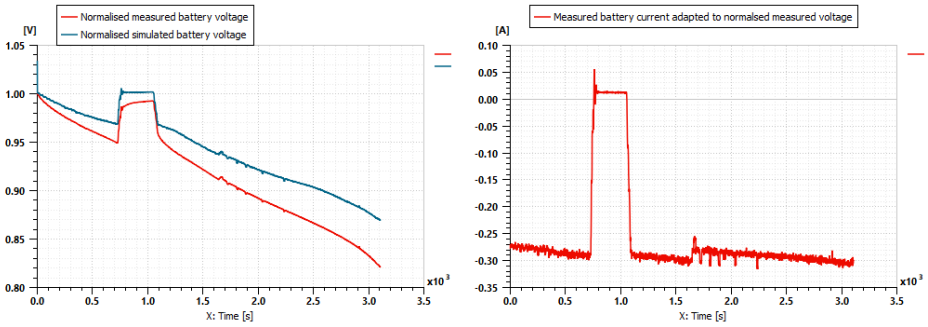

Figure 4.2: *Validation on the normalised battery voltage.*

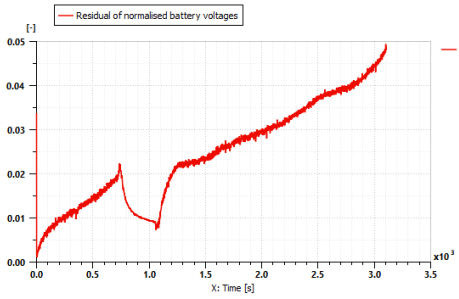

Figure 4.3: *Residual on the battery voltage validation.*

The battery was also validated based on the SOC of the battery during the drive cycle. The SOC from the normalised data collected is plotted against the adapted simulation result in Figure 4.4 as well as the residual is shown in 4.5. From these Figures it can be seen that the collected measurements and the simulated result deviates with time, which is expected due to that the physical battery is aged while the simulation model is based on a new battery.

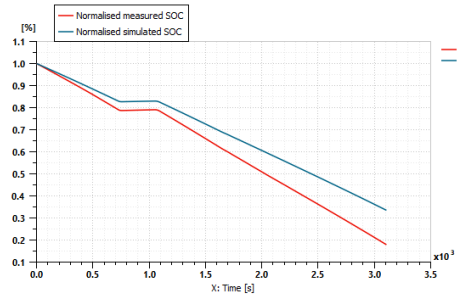

Figure 4.4: *Validation on the normalised SOC of the battery.*

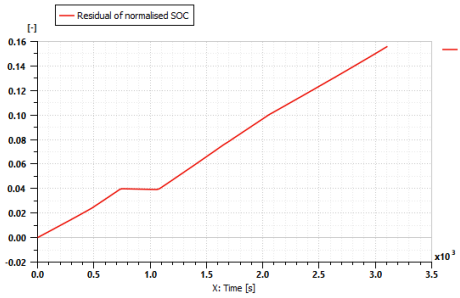

Figure 4.5: *Validation on the normalised SOC of the battery.*

Transmission validation

Before estimating the powertrain inertia and friction, the normalised collected measured data and the normalised simulated rotational speed and the residual is shown in Figure 4.6 where it can be seen that there is both static and dynamic friction difference as well as differences in inertia. The data was collected by measuring the rotational speed at the motor during a test drive at Epiroc's test track and where the AMEsim model in section 3.3.2 was used.

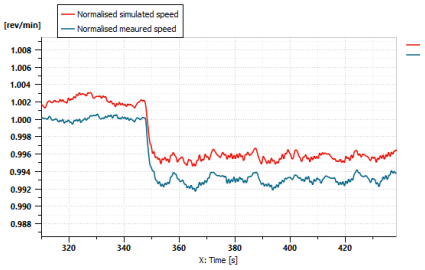

(a) *Normalised measured rotational speed at motor against normalised rotational simulated speed at motor.*

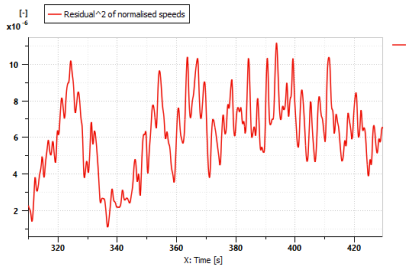

(b) *The square of the residual to the speeds.*

Figure 4.6: *Differences between simulated against measured speed before parameter estimation.*

4.2 Estimating powertrain inertia and friction

The parameter optimisation for inertia and friction was run four times with different starting values by using the method explained in section 3.9.1, two runs was done using genetic algorithm with two different starting values while the other two runs was NLQP with different starting values. The result from this can be seen in Table 4.1. It can be seen that the simulation time is higher when using a genetic algorithm compared to when using a NLPQL algorithm, but the genetic

algorithm results in a lower goal function than NLQP, therefore a more accurate parameter optimisation. It can also be seen that despite different starting values when using a genetic algorithm optimisation, the optimised values are the same, while for NLQP, different starting values results in different results, this is because NLQPL is finding the local optimum and genetic algorithm is finding the global optimum.

Method	Obj. func.	Time	start/stop inertia	start/stop coulomb friction
GA	$2.40 * 17^{-10}$	2h 23 min	500/283	300/492
GA	$2.40 * 17^{-10}$	2h 30 min	20/283	10/492
NLQP	$3.8 * 10^{-6}$	59s	500/466	300/308
NLQP	$9.8 * 10^{-6}$	64s	20/30	10/10

Table 4.1: *Result from Genetic algorithm, GA and NLPQL with different initial values and where the initial values are arbitrary values.*

4.2.1 Parameter estimation using NLPQL optimisation

The parameter estimation using NLQPL is explained in section 2.10.1 and where the result is seen in Figure 4.7 and 4.8. It can also be seen that the search algorithm is not searching for the global value but is finding the local optimum based on the set assumed initial value. The results from method for optimizing the parameters using NLPQL is shown and it can be seen that depending on the initial values, the resulting estimated value is different. It can also be seen that the value has not converged but instead reached a iteration where the La-grangian gradient condition in equation (2.43) have been fulfilled, which means that the solver have found a local minimum solution and therefore stops.

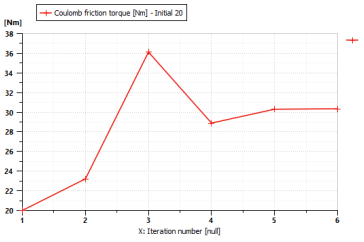

(a) *Start value of 20.*

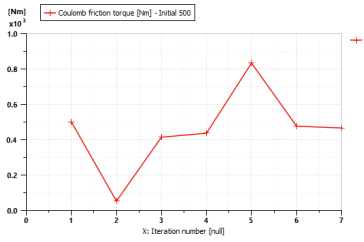

(b) *Start value of 500.*

Figure 4.7: *In (a) the starting value for the NLPQL optimisation of the coulomb friction is 20 while in (b) the start value is set to 500, it can be seen that this methods is only searching for a local optimal value and not a global value.*

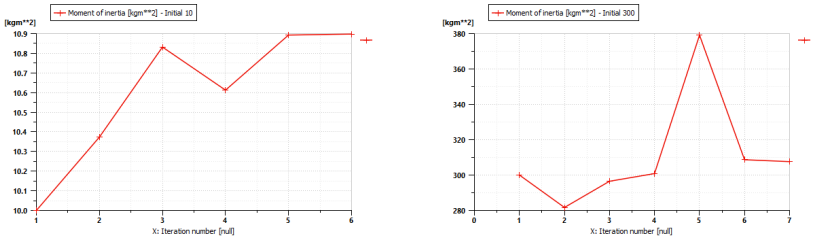

(a) Start value of 10. *(b) Start value of 300.*

Figure 4.8: *In (a) the starting value for the NLPQL optimisation of the inertia is 10 while (b), the start value is set to 300, it can be seen that this methods is only searching for a local optimal value and not a global value.*

4.2.2 Parameter estimation using genetic algorithm

By using a optimisation algorithm explained in section 2.10.2 it is possible to find the values that best fits the actual values. The optimisation process using a genetic algorithm can be seen in Figures 4.9 to 4.12.

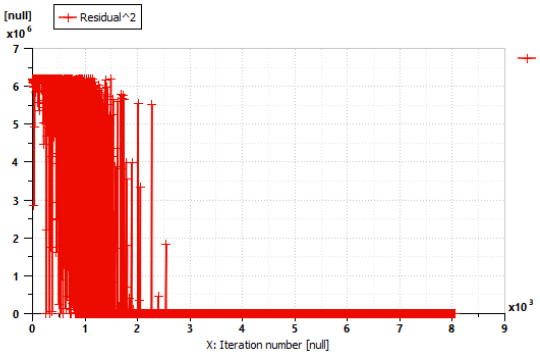

Figure 4.9: *The residual throughout the iterations is converging towards approximately 0, which is the result when the optimisation has found the optimal values for the parameters.*

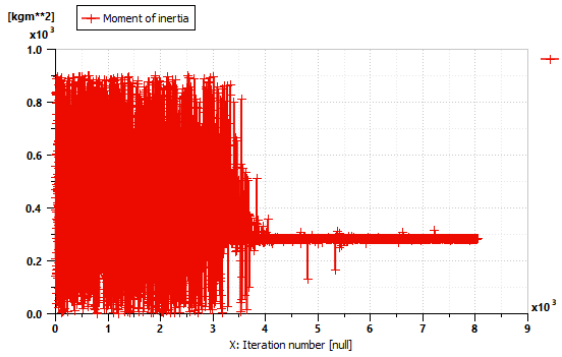

Figure 4.10: *The moment of inertia throughout the iterations are converting converging to a specific value as the search algorithm is trying different values of this parameter.*

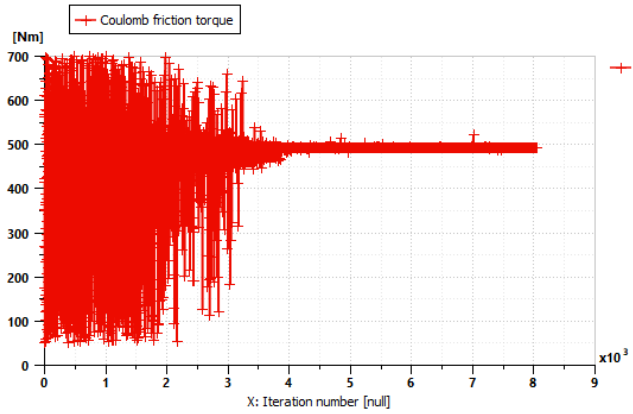

Figure 4.11: *The coulomb friction throughout the iterations are converting converging to a specific value as the search algorithm is trying different values of this parameter.*

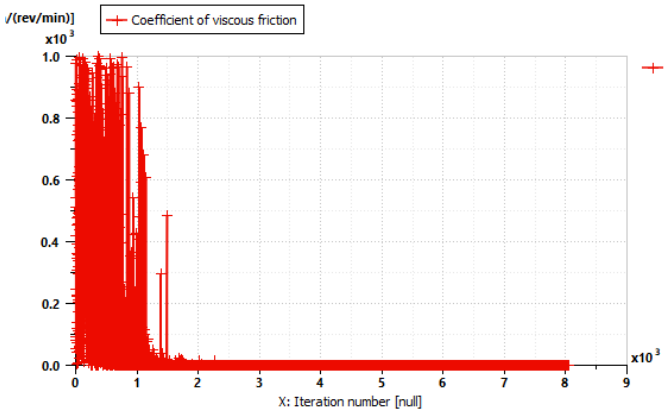

Figure 4.12: *The coefficient of viscous friction throughout the iterations are converting converging to a specific value as the search algorithm is trying different values of this parameter.*

The validation of the transmission box after the parameter optimisation is shown in Figure 4.13 where the measured and simulated rotational speed and the residual is shown and it is seen that the dynamics of the transmission follows the measured data well.

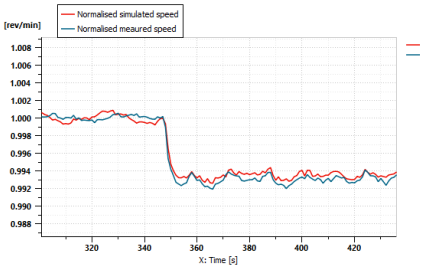

(a) *Normalised measured speed against adapted simulated speed.*

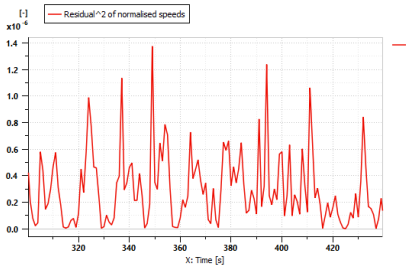

(b) *The square of the residual to the speeds.*

Figure 4.13: *Differences between simulated against measured speed after parameter estimation.*

Validation of torque converter

The validation of the torque converter explained in section 2.6.4 can be seen between the yellow line in Figure 4.14 where the clutch signal is not activated and where the torque converter is activated. The torque converter is activated since the car is accelerating and the extra torque is required. It can be seen that the dynamics of the modelled torque converter matches the dynamics of the data received from the torque converter very well.

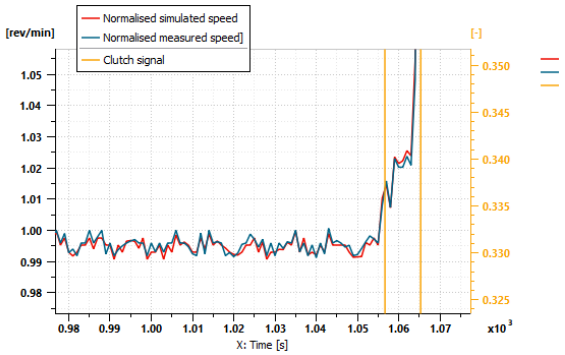

Figure 4.14: *Dynamic validation of torque converter, where it is activated between the yellow lines.*

4.3 AMEsim model for the different motor configurations

In this section the resulting AMEsim model of the centralised motor in section 4.3.1 , axle motor in section 4.3.2, and hub motor in section 4.3.3.

4.3.1 Centralised motor

One of the configurations included in this report is the centralised motor, in this chapter, the result of this choice of motor configuration is shown for the boomer.

AMEsim model with centralised motor

This configuration is implemented in AMEsim as seen in Figure 4.15. In this simulation there is a combination of QSS and dynamic modelling approach, where the electrical subsystem is in QSS and the mechanical in dynamic. The model consists of a driver connected to a controller unit, which is a simple PI controller that controls the requested torque to the motor, a electrical PSMS motor. The model also consist of two gear boxes where the second gear box represents the differential and a vehicle that represents the boomer. There is also an environment setup which represent the road altitude, ambient temperature, and other environmental related settings. Finally there is a power converter to include the efficiency drop from the power electronics, and a battery.

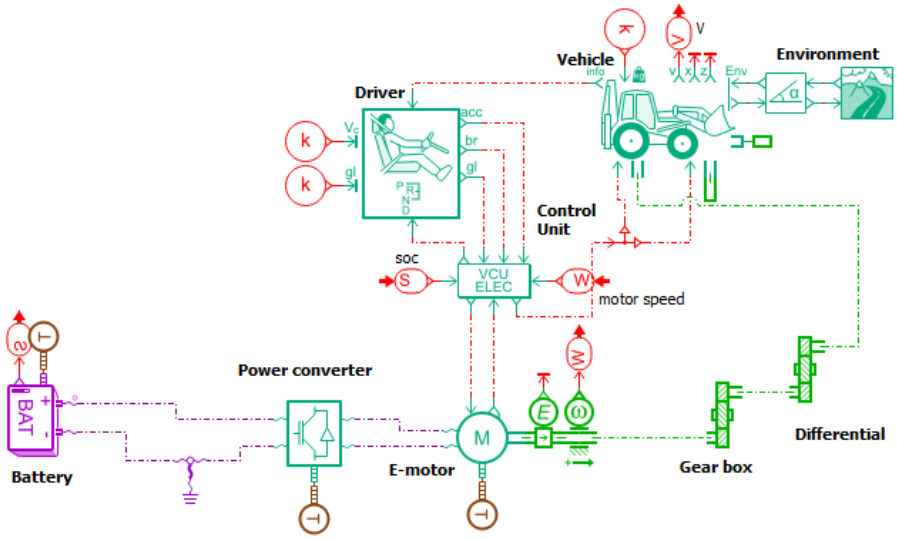

Figure 4.15: *AMEsim model of the centralised motor configuration.*

4.3.2 Axle motor

One of the configurations included in this report is the axle motor, in this chapter, the result resulting model is shown.

Components

Using a axle motor, one motors is placed on the front axle and one on the rear axle resulting in two motors while the transmission including the gear box is no longer included in the vehicle as is explained in section 3.7.

Overview of AMEsim model

The model for the axle motor is very similar as for the centralised motor but now includes another motor and that the gear box is removed. The motors are also connected one to the front wheels and one for the rear wheels.

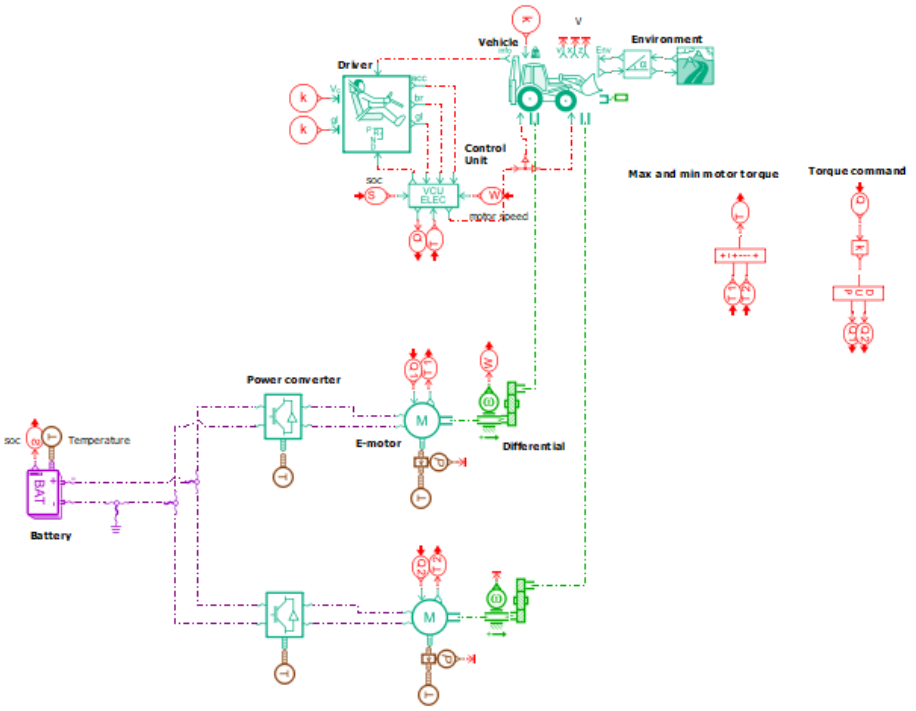

Figure 4.16: *AMEsim model of axle motor configuration.*

4.3.3 Hub motor

One of the configurations included in this report is the hub motor, in this chapter, the resulting model is shown.

Components

In this configuration, the motors are placed on each wheels resulting in 4 motors as well as 4 planetary gears while this also results in the gear box, differential, and axle is removed from the vehicle as is explained in section 3.6.

Overview of AMEsim model

Below in Figure 4.17, the model of the hub motor configurations are shown. The changes done for this model compared to the centralised motor is removing the gear boxes and the differentials and adding three motors, with a gear box for each motor that represents a planetary gear, as well as connecting two motors to the front wheel and two to the rear wheel. The reason for not connecting one motor to each wheel is because of dynamics not being a part of this thesis and therefore this is sufficient for evaluating the energy consumption.

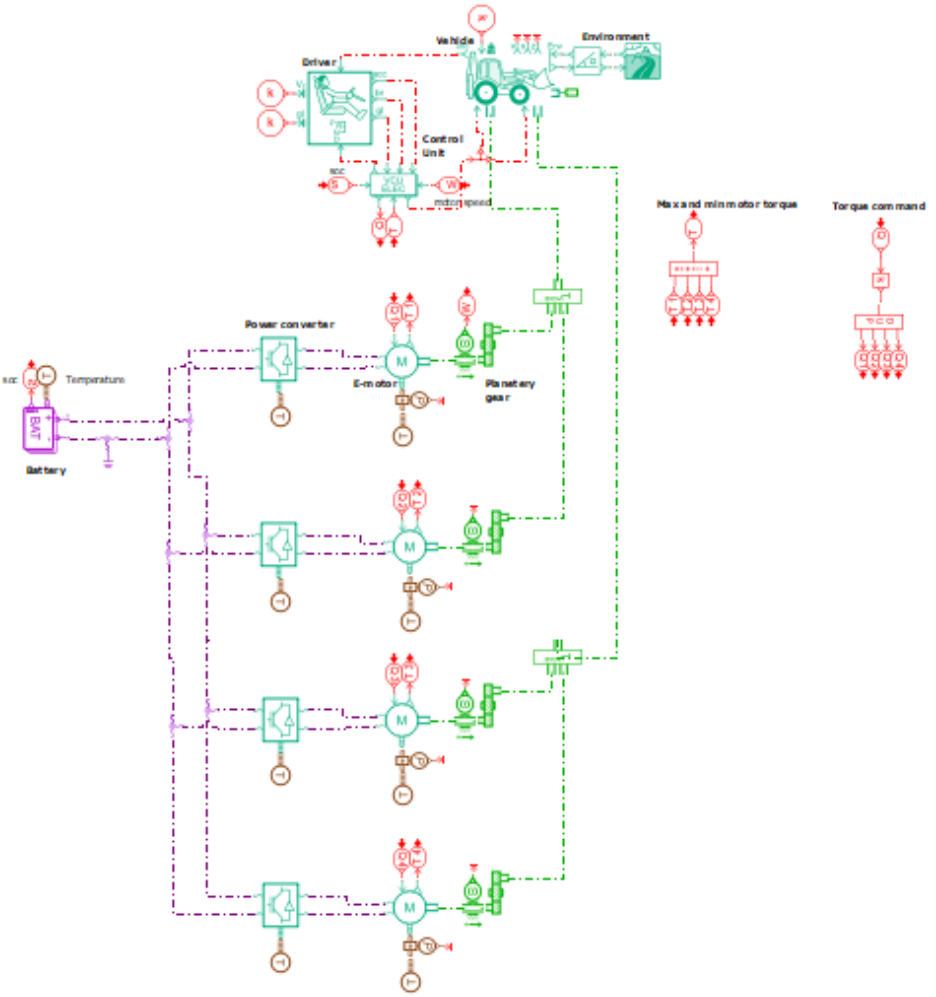

Figure 4.17: *AMEsim model of the hub motor configuration.*

4.4 Sensitivity analyse

The result from the sensitivity analysis explained in section 2.8 is done for the centralised motor configuration and the results are shown in Table 4.2. Comparing the S_P value for the mass with the S_p value for the rolling resistance it can be seen that the change between the old and new value for these parameters is 5.3 times bigger for the change in mass. This means that reducing the mass of the vehicle has a bigger impact on reducing the consumed vehicle energy than reducing the rolling resistance.

Parameter	old/new value	$S_p[-]$
Mass	12000/18000	0.9
Air dynamics	0.5/0.75	0
Wheel inertia	0.5/0.75	0
Rolling resistance	0.03/0.045	0.17

Table 4.2: *Sensitivity analysis.*

4.5 Component optimisation

In this section the result from using optimisation methods for choosing gear ratio for the centralised motor configuration is presented.

4.5.1 Optimizing gear ratio using NLPQL optimisation

In this section an example of the result from optimising the gear ratio for the centralised motor configuration using NLPQL explained in 2.10.1 is shown. The objective function is aiming to minimising the consumed energy as well as increasing the system efficiency. In Figure 4.18 to 4.21 it can be seen how the search algorithm is iterating towards the optimal gear ratio.

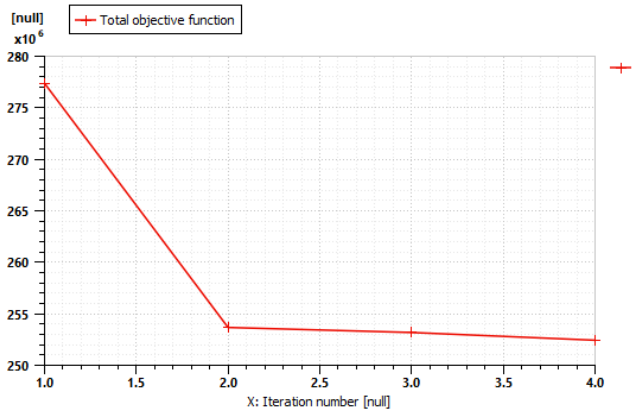

Figure 4.18: *The total objective throughout the iterations as the NLPQL algorithm is searching for the optimal gear ratio for the given goal function and limitations.*

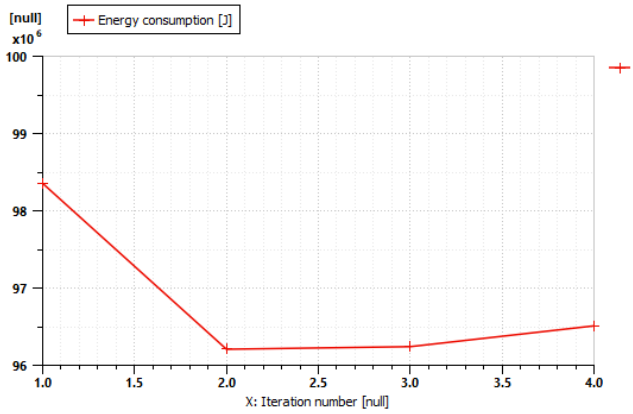

Figure 4.19: *The energy consumption included in the total objective throughout the iterations as the NLPQL algorithm is searching for the optimal gear ratio for the given objective function and limitations.*

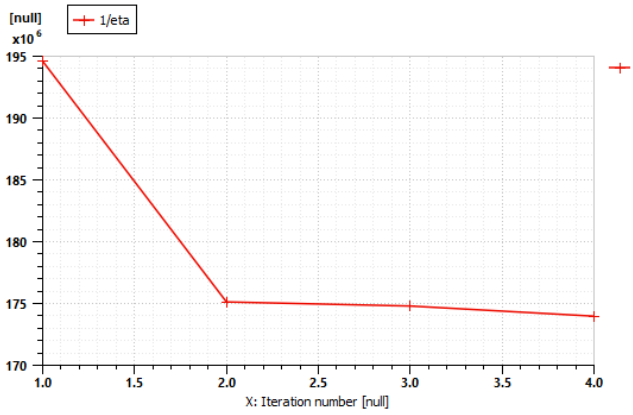

Figure 4.20: *The efficiency factor included in total objective function throughout the iterations as the NLPQL algorithm searching for the optimal gear ratio for the given objective function and limitations.*

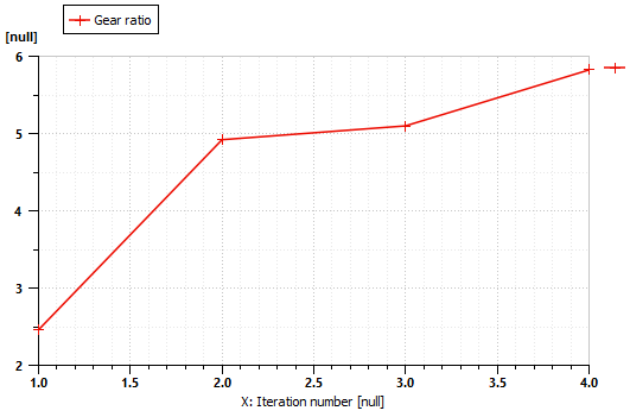

Figure 4.21: *The gear ratio throughout the iteration as the NLPQL is searching for the optimal gear ratio for the given objective function and limitations.*

4.5.2 Impact on optimising the gear ratio

The impact from optimising the gear ratio is shown below in Figure 4.22 to 4.24.

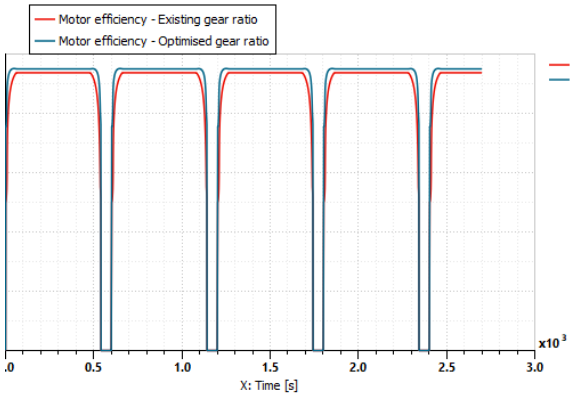

Figure 4.22: *The difference in the motor efficiency between the arbitrary gear ratio compared to the optimised gear ratio.*

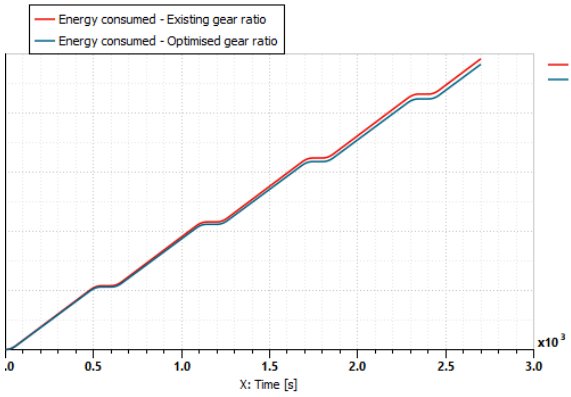

Figure 4.23: *The difference in consumed energy between a arbitrary gear ratio and a optimised gear ratio.*

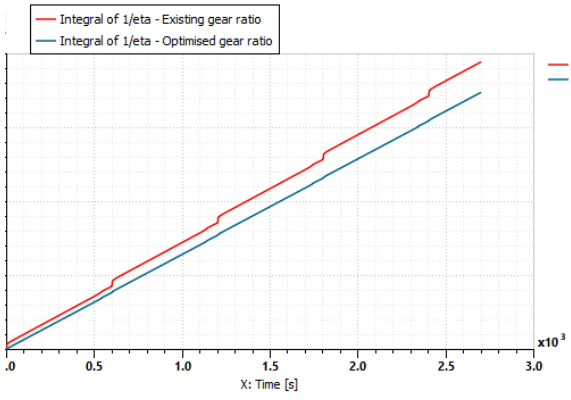

Figure 4.24: *The difference in the efficiency part of the goal function between an arbitrary gear ratio and a optimised gear ratio.*

4.6 Velocity trajectory optimisation

The velocity trajectory optimisation using DDP optimisation methos explained in section 3.10.1 was carried out for two cases where case 1 is for a boomer and case 2 is for an arbitrary vehicle and will be explained in section 4.6.2. Both cases uses a centralised motor configuration and has the same drive cycle shown in Figure 4.25.

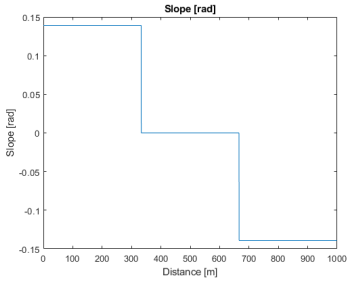

Figure 4.25: *Slope cycle used for both vehicle speed optimisation.*

4.6.1 DDP optimisation for the boomer

In this section the results from using a DDP algorithm for the boomer is presented.

Limitation for DDP optimisation

In Figure 4.26 to 4.28 the power, acceleration and torque used is plotted against the possible max torque that the motor can provide in that instance and where it can be seen that that used torque and power is always kept below or equal to these limitations.

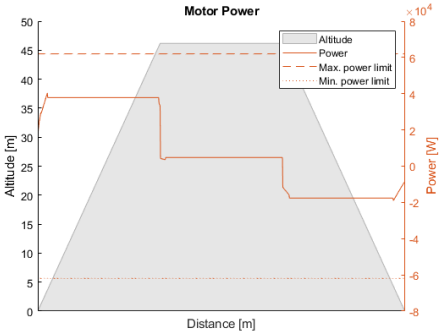

Figure 4.26: Power used vs. power limits.

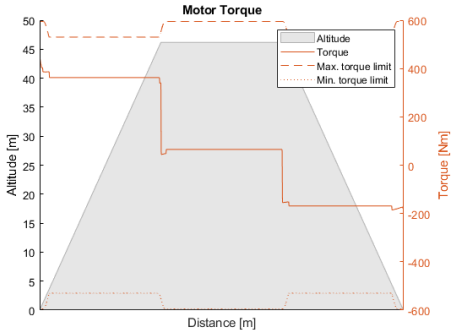

Figure 4.27: Torque used vs. torque limits.

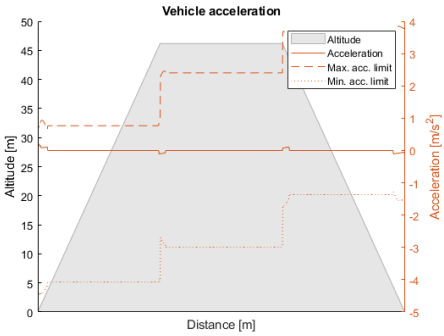

Figure 4.28: Acceleration used vs. acceleration limits.

Optimised speed trajectory for the boomer

The optimisation of the speed trajectory using DDP is done and where the speed trajectory and the resulting SOC can be seen in Figure 4.29 and 4.30. In the SOC curve it can be seen that at the end where the slope is negative, the SOC is increasing, this is because of the generative breaking which charges the battery.

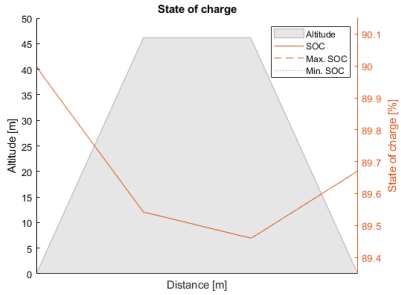

Figure 4.29: *SOC for the DDP optimised vehicle velocity.*

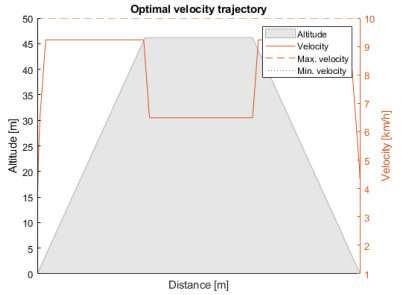

Figure 4.30: *Optimal velocity trajectory obtained from DDP.*

Motor operational points for the boomer

In Figure 4.31, the motor operational points throughout the drive cycle in Figure 4.30 are presented. It can be seen that the operational points for the different slope ranges starts more to the left of the motor efficiency map and then moves to the right as the vehicle accelerates and eventually end up at a certain operational point that is optimal for that slope. It is also possible to see that the operational points for downhill slope has negative torque, this is because of the generative breaking that occurs from driving downhill.

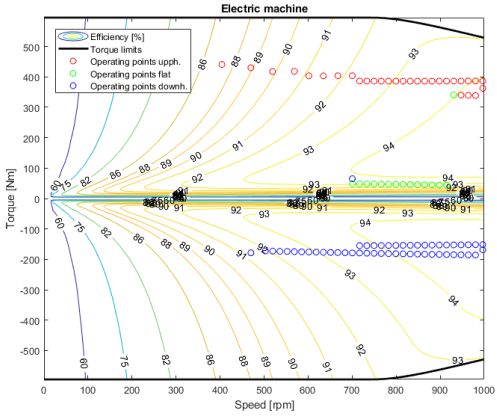

Figure 4.31: *Efficiency map of the electric machine in case 1, illustrating the obtained operational points from the DDP.*

4.6.2 DDP optimisation for an Arbitrary vehicle

In this section the results from using a DDP algorithm for the arbitrary vehicle is presented. The arbitrary vehicle is similar to the boomer but where the parameters such as the vehicle weight and front area are higher as well as replacing

the motor with a motor that has a higher continuous torque and rotational speed. This to evaluate the impact of the DDP for a vehicle that drives at a higher velocity.

Limitation for DDP optimisation

In Figure 4.32 and 4.34 the power, acceleration and torque used is plotted against the possible max torque that the motor can provide in that instance and where it can be seen that that used torque and power is always kept below or equal to these limitations.

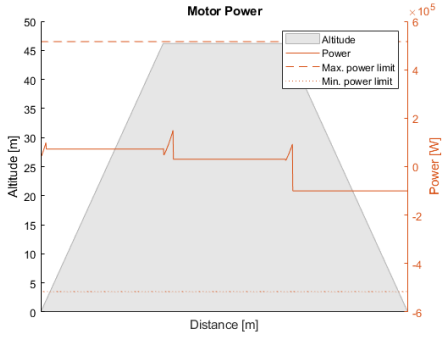

Figure 4.32: *Power used vs. Power limit.*

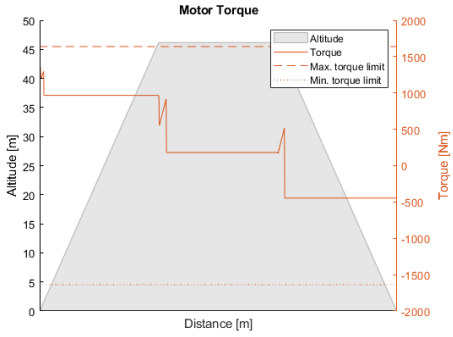

Figure 4.33: *Torque used vs. Torque limit.*

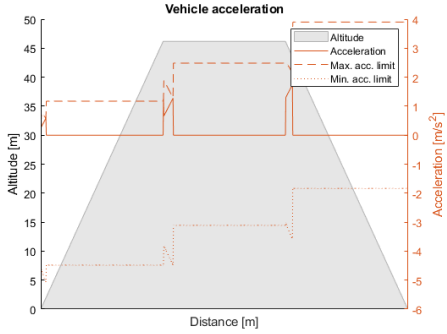

Figure 4.34: *Acceleration used vs. Acceleration limit.*

Optimised speed trajectory for the arbitrary vehicle

The optimisation of the speed trajectory using DDP is done and where the speed trajectory and the resulting SOC can be seen in Figure 4.35 to Figure 4.36. In the SOC curve it can be seen that at the end where the slope is negative, the SOC is increasing, this is because of the generative breaking which charges the battery.

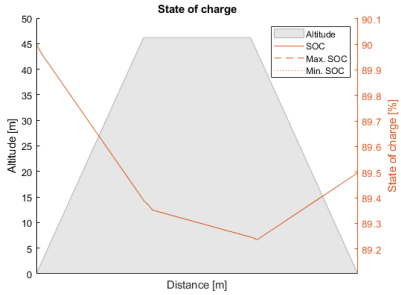

Figure 4.35: *SOC for the DDP optimised vehicle velocity.*

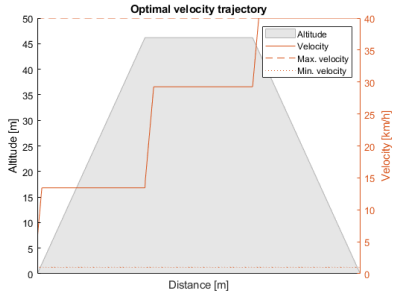

Figure 4.36: *Optimal velocity trajectory obtained from DDP.*

Motor operational points for the arbitrary vehicle

In Figure 4.37, the motor operational points throughout the drive cycle seen Figure 4.36 are presented. It can be seen that the operational points for the different slope ranges starts more to the left of the motor efficiency map and then moves to the right as the vehicle accelerates and eventually end up at a certain operational point that is optimal for that slope. It is also possible to see that the operational points for downhill slope has negative torque, this is because of the generative breaking that occurs from driving downhill.

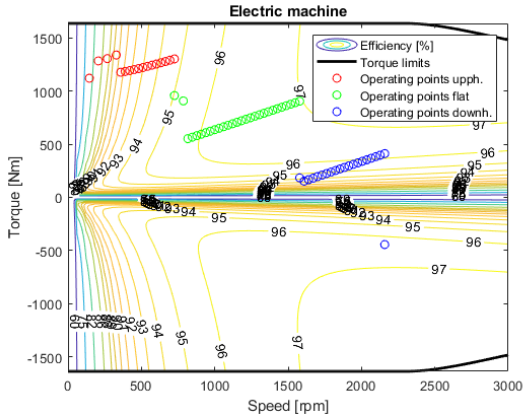

Figure 4.37: *Efficiency map of the electric machine in case 2, illustrating the obtained operational points from the DDP.*

5
Discussion

The discussion chapter contains the reflections and discussions regarding the results obtained in this master thesis. The discussion section consists of a discussion of the results related the AMEsim model in section 5.1.1, the measurement data in section 5.1.2, parameter estimation in section 5.1.3, gear optimisation in section 5.1.4, and vehicle speed optimisation in section 5.1.5.

5.1 Results

The results obtained from this master thesis will be discussed within this section.

5.1.1 AMEsim model

AMEsim is a powerful tool for implementing models easily and offers a wide range of components which also have many characteristics options. By using AMEsim it was possible to create a model that can with good precision match a physical machine. It also provided possibilities to optimise parameters that is difficult to measure in the physical machine.

When validating the transmission, the model and the physical model matched very well, this shows that the genetic optimisation method used to estimate the parameters is a effective way of matching the model with the physical machine. The reason for the small dynamic differences between the model and the physical machine is probably due to measurement noise which is for that purpose neglected when comparing the results. Apart from this transmission, the battery is validated against the actual model where the dynamics is shown to match very

well but it is also possible to notice that the voltage is dropping faster for the physical machine than the model, the reason for this is probably due to aging in the battery used at the physical machine.

5.1.2 Data

To validate the entire model, a lot of measurement data was required that was not possible measured within in this master thesis, such as specific torque values as well as only one suitable operating conditions for validation was given. Therefore only the parts with sufficient data was evaluated while where data was not sufficient, the parameters were set to physically reasonable values. The result from this was that the model is not accurate enough to be used as an example when comparing different powertrain configurations. For example, it was not possible to obtain the measured torque apart from the measured motor torque, therefore the transmission efficiency was not possibly validated and the model can not be modified to match efficiency with the physical machine efficiency. At other places the measurement data was not received at every component but instead measured in the start and end of the transmission, this was the case when validation for example the inertia and the rotational speed,therefore for these parameters the transmission inertia and friction could be validated as a unit but not for each separate component.

The goal of this master thesis was at the beginning to create a AMEsim model for centralised motor, axle motor, and hub motor and compare the energy consumption between the different configurations. Although due to lack of important data, such as data for axle and hub motor as well as measurement data for torque other than motor torque, the aim of this master thesis was changed to instead focus on creating a AMEsim model that can be used to evaluate the different motor configurations once all the required data is obtained. Therefore the focus was to create a AMEsim model for each motor configuration that can easily be modified as well as create tools and methods that can be used to modify the model to match a physical machine, as well as to optimise parameters and vehicle control signals to minimise the energy consumption. A lesson from this is probably to collect and analyse the date before starting a project to then base the project on available date instead of starting the project and then realise that the data is not sufficient for the given task.

5.1.3 Parameter estimation

When estimating the parameters, two different methods were used, the NLPQL algorithm and genetic algorithm. Both of these had their strength and weaknesses when optimising parameters and depending on what is optimised different methods were used. NLPQL is only finding the local optimum, therefore a good understanding of approximate optimal parameter value and objective function is required, in order to implement an initial value relative near global optimum. On

the other hand, the algorithm is significantly faster then the genetic algorithm which is searching for the global optimum. For the genetic algorithm to converge towards the optimum, it presupposes that the settings are arbitrarily well set. For example, a too low value of maximum number of iteration can prevent the algorithm from converging to a value by interrupting the search too early. Using a too small population size can cause you to miss some optimum and therefore it is important to use an arbitrarily large size. It is therefore important to check that the algorithm tests arbitrarily many parameter values, and has enough time to converge towards a certain value provided that an optimum exists. Since NLPQL optimisation is only finding the local optimum, this is better used when there is only one optimum point or if the parameter is easier to calculate. Therefore this method was used when optimising the gear ratio, since this has only one optimal point and therefore NLPQL is sufficient. While for optimising several parameters such as the moment of inertia and frictions combined, then there will be several optimal points, therefore NLPQL might find a local optimum that is not the global optimum, which was the case when the parameter estimation was performed in section 4.2. Changing the relative gradient step or desired gradient accuracy to smaller values in NLPQL increases the accuracy of the optimization, but can not be set so that it searches for only a global optimum. Therefore a genetic algorithm is more suited for this problem, and is the reason why it was used when finding the moment of inertia and the frictions. However, as expected, there was a significantly longer computational time for the genetic in the two optimizations made from the respective initial values when estimating these parameters. For genetic it took 2h 23 min and 2h 30 min respectively while it took 59s and 64s respectively for NLPQL until the optimizations were complete. Genetic is complete when either the maximum number of iterations is executed or until the target function converges to an optimum. NLPQL is complete when the Lagrangian gradient is equal to zero, as described in section 2.10.1.

Another way to find the optimum for objective functions with several local minimums is to combine these two algorithms to save computation time. This is done by first using a genetic algorithm with reduced population size, reproduction ratio and maximum number of generation, i.e, the algorithm converges towards the global minimum area, without finding the absolute best value. With an obtained point reasonably close to global optimum, this can be used as an initial value to NLPQL which then can find global optimum significantly faster than genetic algorithm.

5.1.4 Gear optimisation

The gear objective function for increasing the system efficiency and decreasing the consumed energy for increased gear ratio is a convex function that can be seen in Figure 5.1. This objective function is calculated based on the drive cycle presented in Figure 3.4. Note that since the axle motor configurations do not include any gear, this optimisation can only be implemented to optimise the gear box ratio in the centralised motor configuration and planetary gear ratio in the

hub motor configuration.

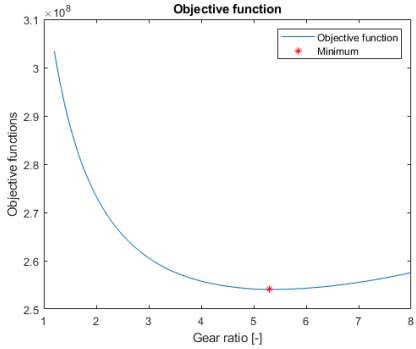

Figure 5.1: *Convex objective function, using Matlab.*

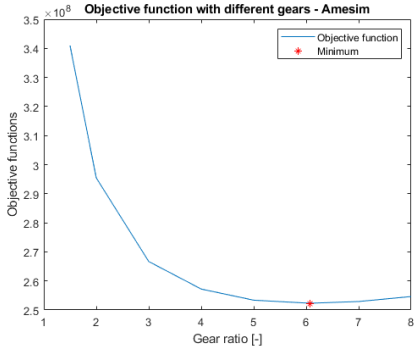

Figure 5.2: *Convex objective function from Amesim.*

When optimising the gear ratio using NLPQL algorithm an optimal gear ratio is found for the given driving cycle. When plotting the objective function for different gear ratios it can be concluded that the method for parameter optimisation based on a objective function is working well. Since the speed trajectory is pre set, the only factor that is impacting the result and therefore the gear ratio is the operating point in the motor. Therefore the NLPQL algorithm is finding the gear ratio that gives the best operational points throughout the drive cycle. If on the other hand, the gear box efficiency would change depending on gear ratio, the objective function would be based on two factors and the result would be a function with several local minimum therefore the use of a genetic algorithm would be better suited to solve this problem.

5.1.5 Vehicle speed optimisation

As seen in the result the speed optimisation is not increasing the energy consumption as much as first thought, this is probably due to the fact that the vehicle speed is low and therefore the counter force created by the wind resistance is not very height. Therefore since the motor efficiency is increasing as the vehicle speed increases, this results in the required increase of required power from the air resistance force being lower than the decrease in power required from a more efficient motor operating point.

Results from DDP

When optimising the speed, the algorithm is finding the best balance between operating at most efficient point at the motor map and minimising the air drag, i.e. minimising the speed. In the first case, when using a smaller motor and driving at lower speed, the speed get more dependent on the efficiency map since the air drag has less impact. It can be seen from the map that the efficiency is increasing when increasing the speed, see Figure 5.3. At lower operating torques in the efficiency map, the speed does not need to increase as much as for higher torque to obtain the same efficiency. This means that at higher operating torques, the speed need to increase more than for lower torques to obtain the same efficiency. This can be seen in the results from case 1, where the torque is relatively high in the uphill and therefore the optimal speed is higher compared when driving at flat road with i.e., lower operating torques. When driving downhill, it is also beneficial to increase the speed as the negative operating torques are higher but also in order to maximise the regenerated power.

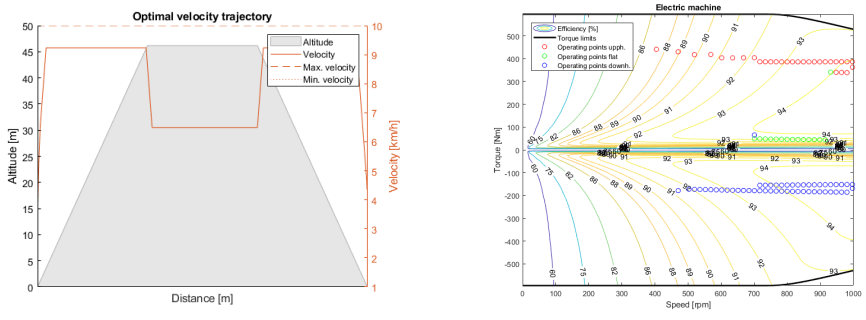

(a) Vehicle velocity trajectory. *(b) Motor operational points.*

Figure 5.3: *Optimal velocity trajectory obtained using DDP in case 1 to the left. Efficiency map and its operational points in blue circles to the right.*

In the second case when using a larger motor, see Figure 5.4 and driving at higher speed, the air drag get an higher impact on the consumed energy, but still

not to the extent that it is the dominant factor for energy consumption. In this case, however, the efficiency map has a slightly smaller impact, as it can be seen that even higher operating torques have a high efficiency at lower speeds, unlike case 1. The reason for obtaining lower speed at uphill and higher speed at downhill is because the consumed energy will decrease at lower speed, while driving downhill, the velocity increases in order to increase the regenerated energy.

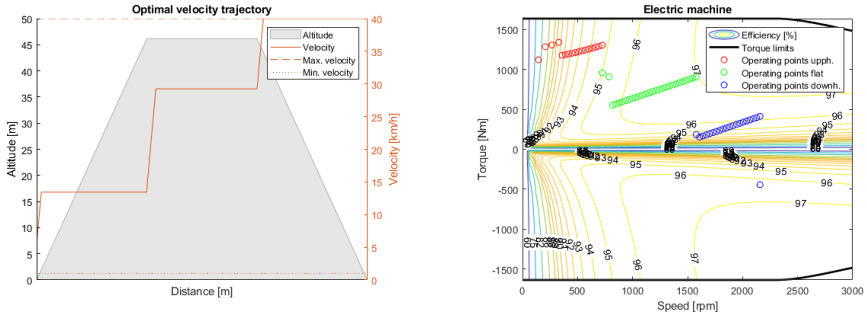

(a) *Vehicle velocity trajectory.* ***(b)*** *Motor operational points.*

Figure 5.4: *Optimal velocity trajectory obtained using DDP in case 2 to the left. Efficiency map and its operational points in blue circles to the right.*

6

Conclusions

This chapter consist of conclusions from the thesis as well as provide further use and development possibilities related to what has been done within this thesis work.

6.1 AMEsim

Creating models in AMEsim is a very good way of creating reliable models that can be used to relatively fast model a physical behaviour that can be used in R&D purposes and at the same time be used to create a visually good model that easily can be used in presentation to project others. With all the inbuilt functions such as dashboard it is very easy to use AMEsim not only as a simulation method but also a easy way to present what is done.

6.2 AMEsim model

There are three problem formulations within this master thesis and where the conclusion drawn from these are shown in this section. The first problem statement is

- Evaluation of how NLQPL and genetic optimisation can be used to estimate unknown model parameters.

The validation of the components or a combination of components can be done by isolating, validating, and modifying to accurately match the physical model. With the use of NLPQL optimization and genetic algorithm unknown parameters could be estimated to accurately match the physical model. With this in mind, this method is a good method to use when creating a model for a physical

machine.

Although the two different optimisation methods that was used for estimating the parameters has different advantages and disadvantages seen in this thesis. Therefore it is important for the user to understand and to decide what method to use based on the model requirement. Since genetic algorithm is computational demanding but searching for global optimum, this is a better option for complex problems with multiple local minimum. On the other hand, if the problem is less complex and have one optimum, NLPQL is a better option since it is less computationally demanding. This can be seen in Table 6.1 where the residual is lower for genetic than NLPQL but is significantly more time demanding.

Method	Obj. func.	Time	start/stop inertia	start/stop coulomb friction
GA	$2.40 * 17^{-10}$	2h 23 min	500/283	300/492
GA	$2.40 * 17^{-10}$	2h 30 min	20/283	10/492
NLQP	$3.8 * 10^{-6}$	59s	500/466	300/308
NLQP	$9.8 * 10^{-6}$	64s	20/30	10/10

Table 6.1: *Result from Genetic algorithm, GA and NLPQL with different initial values and where the initial values are arbitrary values.*

- Evaluation of how NLQPL can be used to when selecting vehicle components to increase the system efficiency and minimise the consumed energy.

A method was created to help developers with parameter selection for components to increase system efficiency and minimise the consumed energy. The method created uses NLPQL optimisation for this parameter selection and where the result shows that NLPQL optimisation increases the efficiency as well as reduces the energy consumption. In the Figure 6.1 it can be seen how the NLPQL method search algorithm is minimising the objective function throughout the iterations.

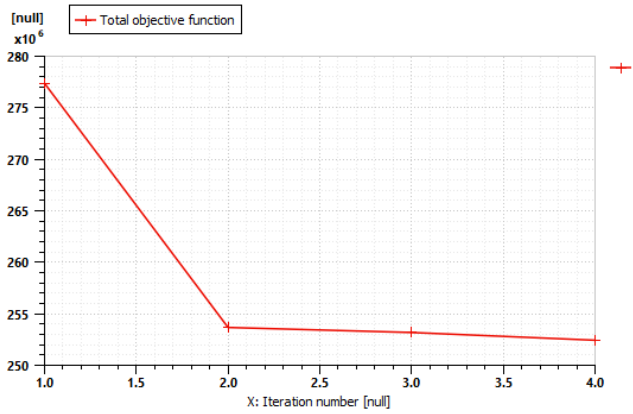

Figure 6.1: *The total objective throughout the iterations as the NLPQL algorithm is searching for the optimal gear ratio for the given goal function and limitations.*

The results from the NLQPL in Figure 6.2 and 6.3 shows a decrease in consumed energy and a increase in the system efficiency. Therefore this method is a good method to use when selecting vehicle components.

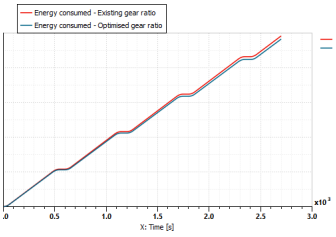

Figure 6.2: *The difference in consumed energy between a arbitrary gear ratio and a optimised gear ratio.*

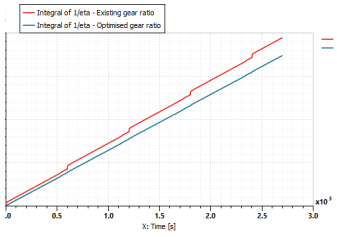

Figure 6.3: *The difference in the efficiency part of the goal function between an arbitrary gear ratio and a optimised gear ratio.*

- Evaluation of how DDP can be used to optimise a control sequence for a drive cycle to increase the system efficiency and minimise the consumed energy.

DDP can be used to optimise the speed trajectory with respect to a cost function that in this thesis contains energy consumption but also penalty factors in order to obtain a desired behavior on the speed. For example, acceleration penalties were used to obtain smoother and more reasonable movements, which gave a satisfactory result on the velocity trajectory. Apart from that, component limitations such as motor maximum torque and motor rotational speed could be implemented to not exceed what is physically possible by the physical machine. This

means that an optimal speed trajectory that both minimises energy consumption and provides a desired behavior can be obtained using DDP. Figure 6.4 show the optimised velocity trajectory for a boomer and an arbitrary vehicle.

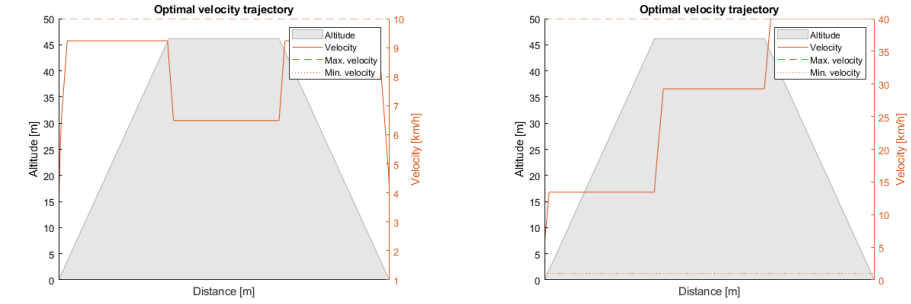

(a) boomer *(b) arbitrary vehicle*

Figure 6.4: *Optimal velocity trajectory obtained using DDP which minimises the energy consumption while providing a desired behavior.*

6.3 Further use and development

The work within this master thesis was focusing on the energy consumption of the vehicle is created as a starting point to further use AMEsim as a simulation method for product development. Therefore there is a lot new to learn within this area and a lot of possible further work. Therefore this section is focused on the possibilities of further work related to energy consumption and different motor configurations.

6.3.1 AMEsim model

The model created is a good model that can be used to evaluate different motor configurations and to therefore understand how the implementation of a new motor will impact the energy consumption and efficiency of the system. But the energy consumption is not the only factor to take into account when deciding between different motor configurations, other aspects such as the vehicle dynamics is a important factor as well. Since this model does not focus on the dynamics of the different motor configurations a way to further develop this model can be to add the dynamics to the model to be able to evaluate the different motor configurations based on both energy consumption as well as other performances parameters.

Another possible way for further work might be to broaden the model to include other parts of the vehicle such as the cooling system and the drill, therefore working towards modelling the entire system and can use that to identify how differ-

ent system work together.

6.3.2 Parameter estimation

The NLPQL optimisation and the genetic algorithm is a good method to more accurately model a vehicle to match the physical model. Apart from that it can be used to optimise product parameters as well as optimise a combination of parameters based on a goal function.

6.3.3 DDP optimisation

Due to low vehicle speed that has approximately the same velocity as the wind, adding the impact on the wind might be a good way to further develop the DDP. It can also be interesting to examine a stochastic dynamic programming where impact such as variation in wind can be a stochastic variable.

Based on what is done within this master thesis it is possible to further develop the DDP as well as use it for different purposes. The DDP model can be modified to optimise other parameters than only the speed. For example it can be used for battery management, or other aspects where optimizing a control signal is beneficial.

6.3.4 Including gear ratio in DDP

Another possible further implementation that can be done is to extent the search grid from the current 2D to a 3D grid, i.e from one degree of freedom (dof) to two dof. The 1-dof grid that is currently implemented is for a vehicle velocity trajectory. Using a 2-dof, it is also possible to for example include a set of gear ratios that can be optimised in combination with the existing vehicle speed. Although this will result in some changes in the model, for example changing gear will probably require a penalty and included in the cost function to not have unrealistic gear changes.

Bibliography

[1] A power change that changes everything. URL https://www.epiroc.com/en-na/innovation-and-technology/zero-emission.

[2] How does internal resistance affect performance? URL https://batteryuniversity.com/article/how-does-internal-resistance-affect-performance.

[3] Jr A. E. Fitzgerald, Charles Kingsley and Stephen D. Umans. *Electric Machinery*. McGraw-Hill, a business unit of The McGraw-Hill Companies, Inc., sixth edition, 2003.

[4] Pratibha Bajpai and Manoj DR. Kumar. Genetic algorithm – an approach to solve global optimization problems. *Indian Journal of Computer Science and Engineering*, 1(3), 2010. ISSN 0976-5166. URL https://www.researchgate.net/publication/283361244_Genetic_Algorithm_-_an_Approach_to_Solve_Global_Optimization_Problems.

[5] Electricalvoice. Genetic algorithm | advantages disadvantages. URL https://electricalvoice.com/genetic-algorithm-advantages-disadvantages/.

[6] Electropedia. Battery and energy technologies. URL https://mpoweruk.com/performance.htm#:~:text=The%20internal%20resistance%20also%20influences%20the%20effective%20capacity,the%20lower%20the%20available%20capacity%20of%20the%20cell.

[7] Tomas Gajdosik, Frantisek Brumercik, Michal Lukac, and Pawel Drozdziel. Vehicle planetary gearbox simulation. *LOGI – Scientific Journal on Transport and Logistics*, 9(1):11–17, 2018. doi: doi:10.2478/logi-2018-0002. URL https://doi.org/10.2478/logi-2018-0002.

[8] Lino Guzzella and Antonio. Sciarretta. *Vehicle Propulsion Systems*. Springer-Verlag Berlin and Heidelberg GmbH Co. K., third edition, 2012.

[9] Prof. Dr. Ronald H.W. Hoppe. Optimization theory. URL https://www.math.uh.edu/~rohop/fall_06/.

[10] YANG LI and MAX SUNDÉN. Modelling and measurement of transient torque converter characteristics. 2016. doi: 10.1051/matecconf/201710001004. URL https://odr.chalmers.se/bitstream/20.500.12380/245130/1/245130.pdf.

[11] Shuai Ma, Modi Jiang, Peng Tao, Chengyi Song, Jianbo Wu, Jun Wang, Tao Deng, and Wen Shang. Temperature effect and thermal impact in lithium-ion batteries: A review. *Progress in Natural Science: Materials International*, 28(6):653–666, 2018. ISSN 1002-0071. doi: https://doi.org/10.1016/j.pnsc.2018.11.002. URL https://www.sciencedirect.com/science/article/pii/S1002007118307536.

[12] Shuai Ma, Modi Jiang, Peng Tao, Chengyi Song, Jianbo Wu, Jun Wang, Tao Deng, and Wen Shang. Temperature effect and thermal impact in lithium-ion batteries: A review. *Progress in Natural Science: Materials International*, 28(6):653–666, 2018. ISSN 1002-0071. doi: https://doi.org/10.1016/j.pnsc.2018.11.002. URL https://www.sciencedirect.com/science/article/pii/S1002007118307536.

[13] Vijini Mallawaarachchi. Introduction to genetic algorithms — including example code. URL https://towardsdatascience.com/introduction-to-genetic-algorithms-including-example-code-e396e98c

[14] Max Olsson. Private interview, March. 25 2022.

[15] Gwangmin Park, Seonghun Lee, Sungho Jin, and Sangshin Kwak. Integrated modeling and analysis of dynamics for electric vehicle powertrains. *Expert Systems with Applications*, 41(5):2595–2607, 2014. ISSN 0957-4174. doi: https://doi.org/10.1016/j.eswa.2013.10.007. URL https://www.sciencedirect.com/science/article/pii/S0957417413008129.

[16] Klaus Schittkowski. *NLPQL*: A fortran subroutine for solving constrained nonlinear programming problems. *Annals of Operations Research*, 5(1), 1986. doi: 10.1007/BF02739235. URL https://www.researchgate.net/publication/225557865_NLPQL_A_FORTRAN_subroutine_for_solving_constrained_nonlinear_programming_problems.

[17] Soumya Sahoo Sushruta Mishra and Mamata Das. Genetic algorithm: An efficient tool for global optimization. *Research India Publications*, 10(8), 2017. ISSN 0973-6107. URL https://www.ripublication.com/acst17/acstv10n8_02.pdf.

[18] Inc. The MathWorks. Genetic algorithm. URL https://se.mathworks.com/discovery/genetic-algorithm.html.

[19] D.J. van Schalkwyk and M.J. Kamper. Effect of hub motor mass on stability and comfort of electric vehicles. In *2006 IEEE Vehicle Power and Propulsion Conference*, pages 1–6, 2006. doi: 10.1109/VPPC.2006.364297.

[20] Ruifeng Zhang, Bizhong Xia, Baohua Li, Libo Cao, Yongzhi Lai, Weiwei Zheng, Huawen Wang, Wei Wang, and Mingwang Wang. A study on the open circuit voltage and state of charge characterization of high capacity lithium-ion battery under different temperature. *Energies*, 11(9), 2018. ISSN 1996-1073. doi: 10.3390/en11092408. URL https://www.mdpi.com/1996-1073/11/9/2408.